Manuscript Details

Manuscript number	MOLLIQ_2018_1133
Title	Deep Eutectic Solvents formed by chiral components as chiral reaction media and studies of their structural properties.
Article type	Full length article

Abstract

We present the realization, the use as reaction media / chiral organocatalysts / acid catalysts and the structural properties of novel chiral Deep Eutectic Solvents. These liquids are formed by mixtures of chiral HBD and HBA molecules that are common, relatively cheap and commercially available (the two enantiomers of camphorsulfonic acid as HBD) or easily one-step synthesized molecules from commercially available compounds ((S)- and (R)-N,N,N-trimethyl-(1-phenylethyl)ammonium methanesulfonate as HBA). These liquids proved to be highly-structured as showed by different yields and enantiomeric excesses observed in a probe reaction, suggesting these liquids to form diastereoisomerically different liquids by changing one of the two enantiomers. Their structural features were analyzed via 1H Pulsed Field gradient Spin Echo (PGSE) NMR, NMR titration, 1H NMR analyses of formation and differences in the chemical shifts of the peaks of the liquids. Density Functional Theory (DFT) optimization helped to define the structures of these liquids. The methanesulfonate counterion of HBA molecule showed to be relevant in order to obtain these highly-structured liquids as it interacts specifically with the HBD. These chiral Deep Eutectic Solvents revealed to be promising novel high-structured media for enantioselective reactions.

Keywords	Chiral Deep Eutectic Solvents; Chiral quaternary ammonium salts; Camphorsulfonic acid; Enantioselective reactions; Structured liquids; NMR analysis.
Manuscript category	Ionic liquids

Corresponding Author	Matteo Tiecco
Corresponding Author's Institution	Department of Chemistry, Biology and Biotechnology, University of Perugia
Order of Authors	Tommaso Palomba, Gianluca Ciancaleoni, Tiziana Del Giacco, Raimondo Germani, Federica Ianni, Matteo Tiecco

Suggested reviewers	Francisco Pena-Pereira, Francois Jerome, Farouq Mjalli, Isabel M. Marrucho, Rafael Chinchilla

Submission Files Included in this PDF

File Name [File Type]

Cover Letter.pdf [Cover Letter]

Highlights.docx [Highlights]

Graphical Abstract.tif [Graphical Abstract]

Manuscript.docx [Manuscript File]

Figure 1.pptx [Figure]

Figure 2.pptx [Figure]

Figure 3.pptx [Figure]

Figure 4.pptx [Figure]

Figure 5.pptx [Figure]

Figure 6.tif [Figure]

Figure 7.tif [Figure]

Scheme 1.pdf [Figure]

Scheme 2.pptx [Figure]

Supporting Information.docx [Figure]

To view all the submission files, including those not included in the PDF, click on the manuscript title on your EVISE Homepage, then click 'Download zip file'.

Perugia, 7/3/2018

Dear Editor,

On behalf of the co-authors I enclose our manuscript entitled "**Deep Eutectic Solvents formed by chiral components as chiral reaction media and studies of their structural properties"** that we would like to submit for publication in Journal of Molecular Liquids.

In this work, we report the studies on novel Deep Eutectic Solvents (DESs) made with chiral components, their properties as reaction media / chiral organocatalysts / acid catalysts and the studies of their structural features. These mixtures derive from common, relatively cheap and commercially available compounds: the two enantiomers of Camphorsulfonic acid as HBD, and easily one-step synthesized molecules from commercially available compounds ((S)- and (R)-*N*,*N*,*N*-trimethyl-(1-phenylethyl)ammonium methanesulfonate) as HBA. These liquids were used in a Michael-type Friedel-Craft probe reaction as active media showing an enantioselectivity that is low but is the same observed in literature with the same reactants in common organic solvents with the addition of chiral organocatalysts. The yields and the enantiomeric excesses observed showed these liquids to be diastereoisomerically different by changing one of the two enantiomers composing them, suggesting these DESs as highly-structured. The NMR studies and the DFT optimizations of their geometries confirmed the multiple sites of interaction between the components of the DESs and also revealed the importance of methanesulfonate counterion in order to obtain these structured liquids.

We believe that due to the novelty of these DESs, to the properties of them, and to the relevance of the observed results, this work can be published in Journal of Molecular Liquids. In literature, to our knowledge, nothing has been published yet on the enantioselectivity determined by the chirality of the molecules forming the DESs; moreover, the NMR techniques used in this paper permitted to obtain relevant data with simple and fast experiments that can be used in future to determine the solubilization of various components of the DESs in various solvents.

The manuscript was written through contributions of all authors. All authors have given approval to the final version of the manuscript. All authors contributed equally. I attest that these results have not been previously published and are not under consideration by any other journal and that all the co-authors are aware of the present manuscript submission.

Best regards

Dr Matteo Tiecco

Deep Eutectic Solvents formed by chiral components as chiral reaction media and studies of their structural properties

Tommaso Palomba, Gianluca Ciancaleoni, Tiziana Del Giacco, Raimondo Germani, Federica Ianni, Matteo Tiecco*

HIGHLIGHTS

- Novel Chiral Deep Eutectic Solvents based on chiral components were realized and characterized.
- Chiral DESs are mixtures of chiral molecules: HBD are common, relatively cheap, commercially available; HBA are easily one-step synthesized.
- Chiral DESs were used as reaction media/chiral organocatalysts/acid catalysts, giving yields and e.e. dependant on the chirality of the components.
- The structural differences between the chiral liquids were studied with NMR techniques and DFT studies.
- The studies revealed these DESs liquids as highly-structured systems.

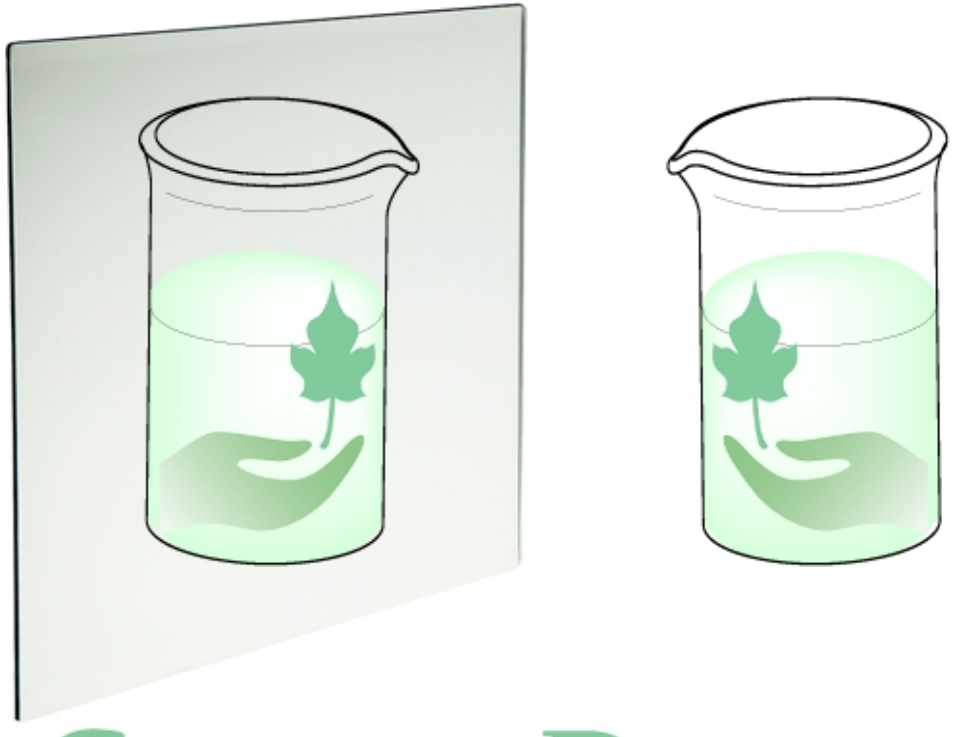

Chiral Deep Eutectic Solvents

Deep Eutectic Solvents formed by chiral components as chiral reaction media and studies of their structural properties

Tommaso Palomba[a], Gianluca Ciancaleoni[b], Tiziana Del Giacco[a], Raimondo Germani[a], Federica Ianni[c], Matteo Tiecco[a]*

[a] Department of Chemistry, Biology and Biotechnology, University of Perugia, Via Elce di Sotto 8 - 06123 Perugia, ITALY.

[b] Department of Chemistry and Industrial Chemistry, University of Pisa, via Giuseppe Moruzzi 13 - 56124 Pisa, ITALY

[c] Department of Pharmaceutical Sciences, University of Perugia, Via del Liceo 1 - 06123, Perugia, ITALY.

* corresponding author. Department of Chemistry, Biology and Biotechnology, University of Perugia, Via Elce di Sotto 8 - 06123 Perugia, ITALY. E-mail: matteotiecco@gmail.com; Tel. +39 075 585 5548; Fax +39 075 585 5560.

ABSTRACT

We present the realization, the use as reaction media / chiral organocatalysts / acid catalysts and the structural properties of novel chiral Deep Eutectic Solvents. These liquids are formed by mixtures of chiral HBD and HBA molecules that are common, relatively cheap and commercially available (the two enantiomers of camphorsulfonic acid as HBD) or easily one-step synthesized molecules from commercially available compounds ((S)- and (R)-*N*,*N*,*N*-trimethyl-(1-phenylethyl)ammonium methanesulfonate as HBA). These liquids proved to be highly-structured as showed by different yields and enantiomeric excesses observed in a probe reaction, suggesting these liquids to form diastereoisomerically different liquids by changing one of the two enantiomers. Their structural features were analyzed via ^{1}H Pulsed Field gradient Spin Echo (PGSE) NMR, NMR titration, ^{1}H NMR analyses of formation and differences in the chemical shifts of the peaks of the liquids. Density Functional Theory (DFT) optimization helped to define the structures of these liquids. The methanesulfonate counterion of HBA molecule showed to be relevant in order to obtain these highly-structured liquids as it interacts specifically with the HBD. These chiral Deep Eutectic Solvents revealed to be promising novel high-structured media for enantioselective reactions.

KEYWORDS

Chiral Deep Eutectic Solvents, Chiral quaternary ammonium salts, Camphorsulfonic acid, Enantioselective reactions, Structured liquids, NMR analysis.

1.INTRODUCTION

Low melting point mixtures that possess green advantages are rapidly increasing their relevance in the recent chemistry, with the aim of reducing the environmental impact of the organic solvents.[1,2] In this field, Ionic Liquids (ILs) have been playing a significant role; in these salts the dispersion and/or the delocalization of the charges lead to poorly coordinating ions and, therefore, to low melting points of the salts (lower than 100°C).[3] ILs have many green properties such as: negligible volatility, high recycle capabilities, low flammability just to mention some of them. For these reasons ILs have been playing relevant roles as reaction and extraction media.[4–6] Moreover, in some chemical reactions these liquids allowed to obtain products otherwise not obtainable with the use of common organic solvents and also easy workup procedures. Unfortunately, these liquids proved to be toxic and resulted low biocompatible because of their low biodegradability.[7–9] Moreover, their synthesis requires synthetic passages involving the use of common organic solvents; therefore, even if these liquids have many advantages compared to typical organic solvents, they still have some green disadvantages.

Deep Eutectic Solvents (DESs) are a new class of organic solvents that can be classified as a sub-class of Ionic Liquids (due to the presence of salts in many of these systems), but they are differently structured and they have many further green advantages compared to ILs.[10,11] Different classifications of these liquids are reported in literature depending on their structures, but they can be simply interpreted as mixtures of a hydrogen-bond donor (HBD) molecule and a hydrogen-bond acceptor (HBA) one at the proper molar ratio.[10,12] These H-bond interactions lead to a decrease of the melting points of these mixtures of molecules, even at room temperature. The syntheses of these systems do not involve the use of any organic solvent because they are prepared by simply mixing and heating two solid compounds until a homogeneous liquid is formed; this is also favourable and “green” in terms of the atom economy of the process.[13]

There are many classes of DESs reported and studied in literature, such as glycerol-based, sugar-based, zwitterion-based ones and so on, with well-defined and unique features and properties.[14–16] A relevant class of these mixtures is represented by Natural Deep Eutectic Solvents (NADES): mixtures of molecules of natural sources, therefore highly bio-compatible, bio-renewable and in many cases cheap.[17–19]

The first and most studied NADES reported in literature is a mixture of choline chloride and urea at 2:1 molar ratio.[20,21] In this case the H-bond interactions occurring between the hydrogens of urea and the chloride counterion of choline lead to a decrease of the electrostatic interactions

between the ammonium and the chloride itself, provoking a high decrease of the melting point of the mixture (m.p. Urea = 134°C; m.p. Choline Chloride = 302°C; f.p. DES (Choline Chloride/Urea) = 12°C).

Beside the green preparation procedures of these liquids, recent studies also showed that these mixtures are non-toxic, biodegradable and biocompatible; this is also more relevant in the case of the NADES due to the natural origin of the molecules composing them.[22–25] As a significant example, Choline chloride / Glycerol mixture was recently studied as non-toxic drug carrier in living organisms.[26]

For these reasons DESs are rapidly increasing their relevance in the green chemistry literature; their application is wide and concerns solvents for organic synthesis, extraction media, media for the synthesis of nanoparticles, electrochemistry, biocatalysys, and so on.[27–33]

DESs represent a novel step forward in the green chemistry, and many topics about these liquids are yet to be explored. The step forward in this topic is represented by the use of smart DESs: solvents that could play an active role (such as a catalytic one) in the reaction or in the process where they are applied. Their use as reaction media/organocatalyst for enantioselective reactions and the study of the properties of chiral DESs is still lacking. Recently Ñíguez, Guillena and Alonso published a work about the dissolution of a chiral organocatalyst in a choline chloride/glycerol mixture that led to interesting results;[34] an enantioselective L-proline catalyzed inter-molecular aldol reaction was successfully performed in various DESs by Martìnez and co-workers[35]; high stereo- and enantioselective additions were performed dissolving a chiral amine in choline-based DESs[36]. However, the chirality of the DES itself, and its effect in the asymmetric synthesis topic, is yet to be explored.

This topic has already been studied and interpreted in Ionic Liquids literature; there are many works about the dissolution of chiral auxiliaries in these media and also about the functionalization of classic Ionic Liquids with chiral auxiliaries branches.[37–41] In these works, a low enantioselectivity induction is reported using liquids made of chiral molecules with non-specific interactions with the reagents.[37,42] The specific interactions of the reagents with the chiral auxiliary, or with the supported chiral auxiliary, is in fact a key-factor in order to obtain a good enantioselectivity in a chemical reaction or an effective chiral recognition.[43,44]

In this work, we present the realization and the structural characterization of novel Chiral Deep Eutectic Solvents based on the combinations of both enantiomers of chiral HBD and HBA molecules. The molecules used in this work as chiral HBD were the two enantiomers of Camphorsulfonic acid

((1R)-(-)-10-Camphorsulfonic acid and (1S)-(+)-10-Camphorsulfonic acid, -CSA and +CSA); the HBA molecules were the two enantiomers of *N*,*N*,*N*-trimethyl-(1-phenylethyl)ammonium methanesulfonate (FR and FS), easily synthesised in one step from the corresponding primary amines. All these compounds are cheap and they are commonly used as chiral resolution reagents. We successfully used these novel chiral liquids as reaction media / chiral organocatalysts / acid catalysts in a Michael-type Friedel-Crafts addition probe reaction. The structural features of these liquids were studied via different NMR techniques; besides molecular modelling studies were performed to obtain a structural interpretation of the data.

The chirality of the molecules composing the liquid mixtures revealed to be necessary but not sufficient to obtain a significant enantiomeric excess in the probe reaction, so suggesting these DESs as highly-structured liquids. As confirmation of this, no enantiomeric excesses were observed with liquids with non-chiral components, and different yields and different enantiomeric excesses were observed for the mixtures with the same enantiomer of the HBD but with the two enantiomers of the HBA (+CSA/FR and +CSA/FS). All these data suggested the existence of diastereoisomerically different liquids made with different enantiomer couples. This was proved via different NMR studies. NMR diffusion data revealed a marked self-aggregation process in chloroform, leading to the existence of clusters of about four HBD/HBA couples. The observed association constants were different for the diastereoisomerical different liquids. The ^{1}H-NMR analysis revealed differences in the DESs formation ($\Delta\delta_{form}$, shifts of the signals between the DES and the pure compounds, δ_{DES} - $\delta_{pure\ compounds}$) and between the two DESs ($\Delta\delta_{DESs}$ = shifts of the signals between two different DESs mixtures) in all the combinations of the enantiomer couples, with a correlation between the differences of the yields (Δ_{yields}) in the two liquids in the studied Michael addition with the differences of the chemical shifts ($\Delta\delta_{DESs}$) of the ^{1}H-NMR spectra. Finally, the geometry of the various adducts have been optimized by Density Functional Theory in order to obtain a hypothesis of the structures of these novel liquids.

2.RESULTS AND DISCUSSION

2.1 DESs PREPARATION AND USE AS CHIRAL MEDIA

2.1.1 DESs preparation

The first step of this work was the preparation of the chiral HBA molecules; the HBD (the two enantiomers of Camphorsulfonic acid, +CSA and -CSA) are in fact commercially available.

Quaternary ammonium methanesulfonate HBA molecules were chosen in a set of differently structured molecules that we recently had developed in order to obtain halogen-free DESs.[12,15,25,45] (R)- and (S)-*N*,*N*,*N*-trimethyl-(1-phenylethyl)ammonium methanesulfonate (FR and FS) were synthesised in one step from the correspondent primary amines via reaction with methyl-methanesulfonate in good yields (over 80%). These solids (m.p. = 166-168°C) were separately mixed with +CSA (m.p. = 198°C) and heated at molar ratio 1:1 to give viscous liquids with low freezing points (20°C) (Scheme 1).

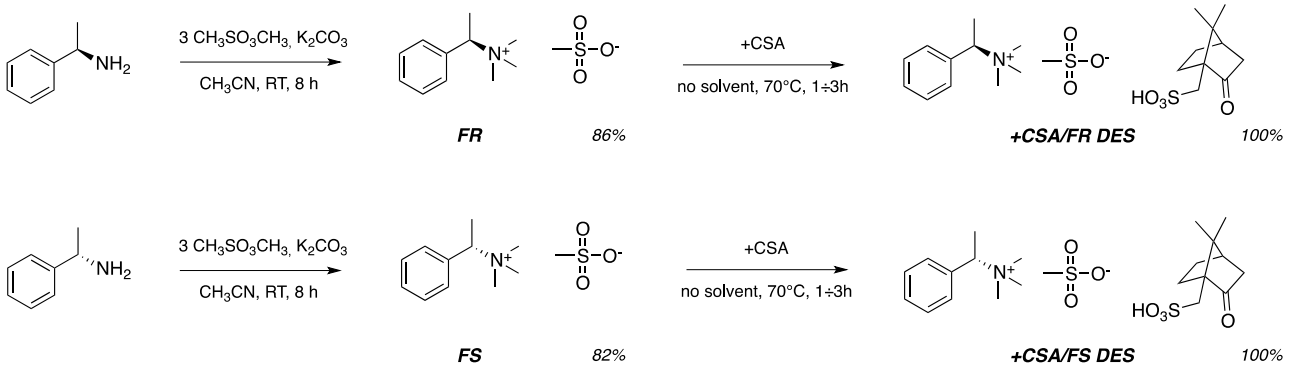

Scheme 1: Chiral DESs realization: synthesis of (R)- and (S)-N,N,N-trimethyl-1-phenylethanaminium methanesulfonate (FR and FS) via methylation of the primary amines; mixtures with (1S)-(+)-10-Camphorsulfonic acid to give the DESs.

In supporting information section (Figure S1) the eutectic profiles of these mixtures, depending on the molar ratios, are reported. The HBD:HBA molar ratios used in this work were all 1:1, also because the melting points vary very little changing the composition of the mixtures; at these molar ratios, the freezing points of the liquids with all the combinations of the two enantiomers of CSA and of the two quaternary ammonium salts were measured (also with racemic mixtures) and they were all about the same values (between 21°C and 17°C, see supporting information (Table S1).

2.1.2 Use of the novel chiral DESs in Michael-type Friedel-Crafts probe reaction addition

The novel liquids were used as media/active DESs in a Michael-type Friedel-Crafts probe reaction of addition of indole to chalcone. This addition was chosen as a probe reaction because it is simple and fast; the reactants are cheap and the reaction has been studied in literature in different solvents with the addition of +CSA as chiral Brønsted acid catalyst to promote enantioselective addition to the double bond of chalcone (Scheme 2).[46]

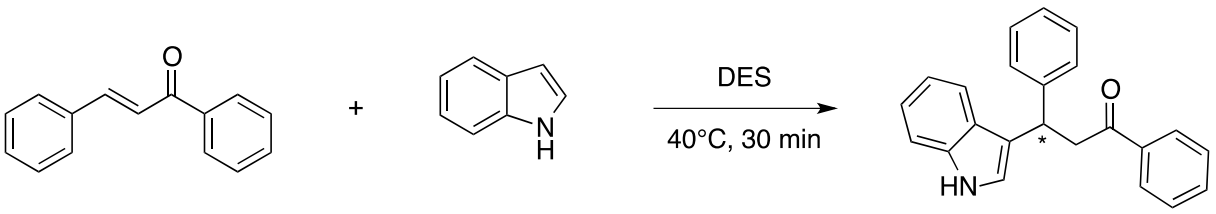

Scheme 2: Michael-Type Friedel-Crafts reaction of indole to chalcone in chiral DESs.

This reaction showed different yields (spanning from 33 to 98%) and enantiomeric excesses (spanning from 0 to 20%) depending on the solvent used as reported in literature.[46] In our case, the mixtures +CSA/FR and +CSA/FS act simultaneously as green reaction media, chiral organocatalysts and acid catalysts for this reaction. In order to homogenize the data with the ones of our liquids (in terms of the amounts of +CSA in the mixtures) and in order to reduce the viscosity (and therefore increase the solubility of the reactants in the mixtures), the first experiment was to increase the temperature (up to 40°C) of the literature reaction in CH_3CN and the addition of equivalents of +CSA (4:1 molar ratio with the solvent). Our DESs, in fact, are highly viscous at room temperature and their viscosity rapidly decreases increasing the temperature up to 40°C. The reaction times were set at 30 minutes for all the samples. In these conditions, the yield observed in CH_3CN was 90% and the enantiomeric excess (e.e.) was 10%. Using our two novel chiral-DESs we observed different yields and different e.e. between the two liquids: 82% yield and 11% e.e. in +CSA/FR and 45% yield and 5% e.e. in +CSA/FS (Table 1).

Table 1: Yields and e.e. observed for the addition of Indole to Chalcone in different media: CH_3CN with +CSA (4:1 molar ratio); +CSA/FR DES; +CSA/FS DES[a].

Solvent	Yield (%)	e.e. (%)
CH_3CN/+CSA (4:1)	90	10
+CSA/FR DES	82	11
+CSA/FS DES	45	5

[a] Reaction time = 30 minutes at 40°C. Yields calculated via weighted product after column chromatography. Enantiomeric excesses (e.e.) calculated via HPLC with chiral stationary phase.

These data suggested to explore the use of further differently structured Deep Eutectic Solvents for a better interpretation. In order to evaluate the role of the chiral components in the reaction, first we performed the reaction using combinations of chiral and non-chiral HBD and HBA components: *p*-toluensulfonic acid (PTS) was used as non-chiral HBD molecule, and N,N,N-trimethylcyclohexylammonium methanesulfonate (CyAMes) and N,N,N-trimethylbenzylammonium methanesulfonate (BnAMes) were used as non-chiral HBA molecules with high structural similarity with FR and FS. In Table 2 all the yields and the e.e. observed for these systems are reported.

Table 2: Yields and e.e. observed in the reaction of chalcone with indole in different media: CH_3CN/+CSA and in the novel DESs made with combination of chiral (*) and non-chiral HBD and HBA molecules.[a]

	Solvent	Yield (%)	e.e. (%)
NO DES	CH_3CN/+CSA (4:1)	90	10
HBD*/HBA* DES	+CSA/FR	82	11
	+CSA/FS	45	5
HBD*/HBA DES	+CSA/CyAMes	81	6
	+CSA/BnAMes	52	4
HBD/HBA* DES	PTS/FR	58	2
	PTS/FS	85	2

[a] Reaction time = 30 minutes at 40°C. Yields calculated via weighted product after column chromatography. Enantiomeric excesses calculated via HPLC with chiral stationary phase.

The yields observed in those media were different, suggesting diastereoisomeric differences between the liquids; the enantiomeric excesses are significant only in the mixture +CSA/FR, while with the other DESs are small. The couples +CSA/FR and +CSA/FS showed different enantiomeric excesses and different yields, suggesting these media as diastereoisomerical different liquids.

The step ahead was then to realize and study the reactivity of all the possible enantiomeric combinations of +CSA and -CSA and the FR-FS couples, considering also their racemates (±CSA and FRS) and their combinations with the pure enantiomers. The results are reported in Table 3.

Table 3: Yields and enantiomeric excesses observed in the reaction of chalcone with indole in different DESs made with combinations of the two enantiomers of Camphorsulfonic acid (+CSA, -CSA), the two enantiomers of N,N,N-trimethyl-(1-phenylethyl)ammonium methanesulfonate (FR and FS) and their racemates (±CSA and FRS).[a]

DES	Yield (%)	e.e. (%)
+CSA/FR	82	11
+CSA/FS	45	5
-CSA/FR	66	<2
-CSA/FS	54	<2
±CSA/FR	66	<2
±CSA/FS	64	4
+CSA/FRS	59	<2
-CSA/FRS	48	<2
±CSA/FRS	51	<2

[a] Reaction time = 30 minutes at 40°C. Yields calculated via weighted product after column chromatography. Enantiomeric excesses calculated via HPLC with chiral stationary phase.

From these data emerged that the enantiomeric excesses are relevant only for one of the combinations of HBD/HBA molecules: +CSA/FR mixture. The value is almost identical to the one of CH_3CN with +CSA and is similar to the reactions in toluene and dichloromethane at room temperature as reported in literature.[46] The different yields observed suggest these mixtures to be diastereoisomerically different even if they differ only in one chiral center of the two molecules. These data suggest these mixtures as highly structured liquids, and that the H-bonds interactions are not the only ones that can occur in these systems.

The differences in these liquids were analyzed first via different NMR techniques in $CDCl_3$ solutions, in order to obtain structural information of the systems. Chloroform was chosen as a non-protic apolar solvent, in order to solubilize the molecules and not to interfere with the H-bonds in the DESs structures.

2.2 STRUCTURAL PROPERTIES OF THE CHIRAL DESs

2.2.1 ^{1}H Pulsed Field gradient Spin Echo (PGSE) NMR

The supramolecular aggregation of the DESs in $CDCl_3$ has been investigated by means of ^{1}H Pulsed Field gradient Spin Echo (PGSE) NMR.[47,48] In fact, it is known that ammonium salts dissolved in organic solvents can give a complex mixture of ionic couples and/or clusters, whose size and composition depend not only on the solvent polarity, but also on the nature of cation and anion, and the hydrophobic portions.[49]

Firstly, the hydrodynamic volumes of the single components have been evaluated. In $CDCl_3$ +CSA shows a hydrodynamic volume (V_H^0) of 205 Å^3 at 35 mM. On the other hand, FS is a salt and its V_H could be function of the concentration.[49] Indeed, V_H(FS) resulted to be 551 and 466 Å^3 at 28.4 and 1.5 mM, respectively. Consequently, the hydrodynamic volume of the adduct +CSA/FS, V_H^0(+CSA/FS), can be calculated to be 205 + 466 = 671 Å^3. Evidently, V_H^0(+CSA/FR), is the same.

The possibility of a higher aggregation has been evaluated dissolving the pre-formed DES directly in $CDCl_3$, in order to strictly maintain the 1:1 molar ratio between the two components at all the concentrations, and measuring the trend of V_H with +CSA/FS or +CSA/FR. As shown in Table 4, in both cases all the V_Hs show a marked tendency to increase as the concentration increases, denoting a clear aggregation process. In particular, for +CSA/FS, V_H(FS) spans between 792 and 2933 Å^3 at 4 and 234 mM, respectively. At the same concentrations, V_H(+CSA) goes from 613 to 2943 Å^3, respectively. The fact that V_H(+CSA) is systematically slightly smaller than V_H(FS) is not easy to explain, for the presence of many equilibria in solution: the ion pairing process of FS, the formation of the supramolecular anion [methanesulfonate*+CSA]$^-$, its ion pairing process with [(S)- *N*,*N*,*N*-trimethyl-(1-phenylethyl)ammonium]$^+$ and the self-aggregation properties of each of these aggregates. Anyway, the fact that V_H(+CSA) and V_H(FS) increase at the same rate strongly suggest that they are part of the same aggregate.

The case of +CSA/FR is quite similar, giving comparable values of V_Hs at all the studied concentrations.

The number of aggregation N, defined as V_H(FS), or V_H(+CSA), divided by V_H^0(+CSA/FS), allows a quantitative estimation for the aggregation, indicating how many HBA/HBD "couples" are present in an average supramolecular adduct.

Table 4: Diffusion coefficients (D_t, 10^{-10} m^2s^{-1}) and hydrodynamic volumes (V_H, Å^3) of (+CSA/FS) and (+CSA/FR) in $CDCl_3$ at different concentrations (C, mM).

C (+CSA/FS)	**D_t(FS)**	**D_t(+CSA)**	**V_H(FS)**	**V_H(+CSA)**	**N(FS)**	**N(+CSA)**
4	7.41	8.28	792	613	1.2	0.9
21	5.69	6.12	1537	1277	2.3	1.9
95	4.96	5.10	2218	2050	3.3	3.1
234	4.47	4.46	2933	2943	4.4	4.4
C (+CSA/FR)	**D_t (FR)**	**D_t (+CSA)**	**V_H(FR)**	**V_H(+CSA)**	**N(FS)**	**N(+CSA)**
10	7.07	7.59	891	751	1.3	1.1
100	4.95	5.11	2226	2049	3.3	3.0
185	4.53	4.59	2825	2739	4.2	4.1

The presence of four couples of HBD/HBA molecules in these solutions at these concentrations is relevant, as they can represent a system that could be more similar to the pure liquids compared with the solutions of single couples of HBD/HBA. Plotting the trends of the aggregation numbers *vs.* the concentration, the similarity of the two systems +CSA/FR and +CSA/FS can be easily appreciated (Figure 1).

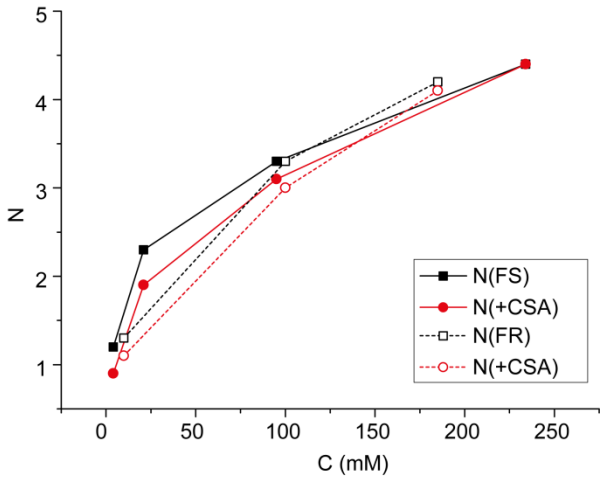

Figure 1: Trend of the aggregation numbers for +CSA/FS (filled symbols) and +CSA/FR (empty symbols).

2.2.2 ^{1}H-NMR titrations

The interaction between the two components of the DES has been investigated through ^{1}H NMR titrations in $CDCl_3$,[50] keeping the concentration of FS or FR constant and progressively increasing [+CSA]. Fitting the experimental data for the -CH- in the chiral center, the formation constants (K_f) of the two DESs resulted to be 131 and 115 M^{-1} for +CSA/FS and +CSA/FR, respectively. The two values are similar, but not equal, denoting a slightly different interaction between the units in the two diastereoisomeric couples. All the data are reported In Supporting Information section (Table S2-S3 and Figure S13).

2.2.3 ^{1}H-NMR Spectra Studies

The couples +CSA/FS and +CSA/FR DESs were studied in chloroform-d solutions at the concentration of 203 mM (0.1 g/mL). This value was chosen because the systems HBD/HBA are present in four couples at these concentrations as emerged from PGSE experiments. The chemical shifts ($\Delta\delta_{form}$ =

δ_{DES} - $\delta_{pure\ compounds}$) between the same signals in the DESs mixtures compared to the ones of the pure compounds were studied. These data gave us structural information on the different liquids structures. The DESs couples +CSA/FR and +CSA/FS were analyzed in detail with this approach as they represent the most relevant couple in terms of observed differences. In Figure 2 are reported the stacked ^{1}H-NMR spectra of FS, of +CSA and of the +CSA/FS DES. The stacked spectra of +CSA, FR and the +CSA/FR DES and all the data of all the systems are reported in Supporting Information section (Figure S13, Table S4-S5).

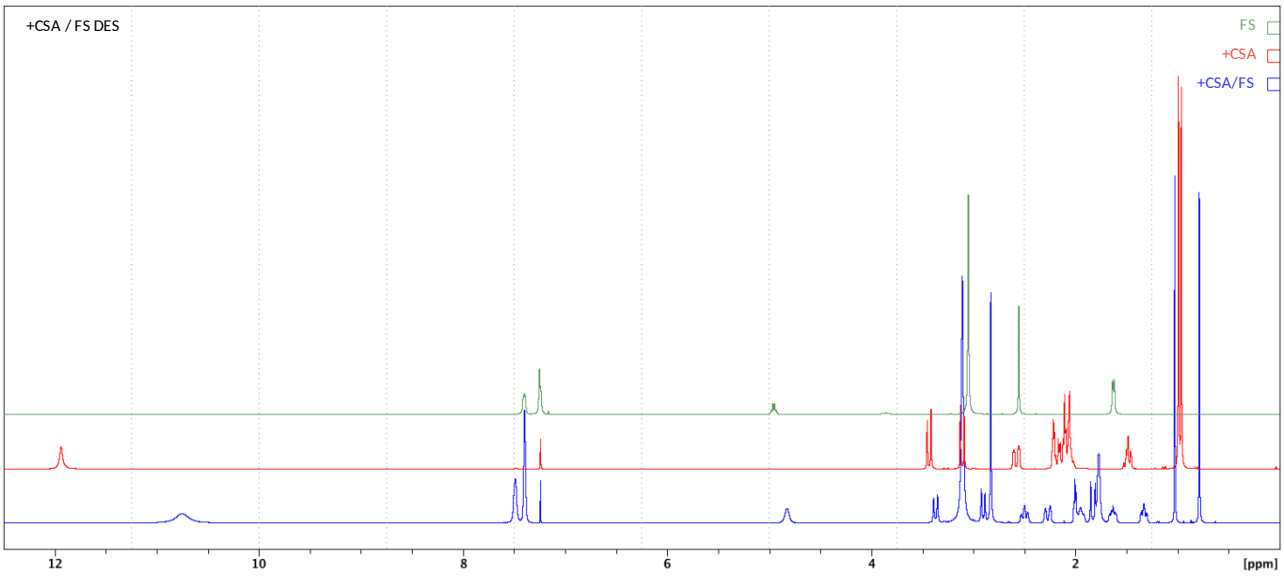

Figure 2: Stacked ^{1}H-NMR spectra in $CDCl_3$ of FS (green), +CSA (red) and the +CSA/FS DES (blue) in $CDCl_3$. All the spectra were calibrated on the solvent signal.

Shifts of the signals were observed in all the analyzed samples passing from the pure components to the DESs. To ensure these data were not only due to the concentration of the components, concentration profiles were analyzed (see supporting info Figure S14) and these spectra show all the peaks shifting in the same direction as the concentration of the samples changes. In these experiments the $\Delta\delta_{form}$ have different signs. In CSA, a shielding effect on the signals was observed for almost all the peaks, with two peculiar signals: the geminal -CH_3 signals are more separated in the DESs (0.2396 ppm in DES, 0.0279 ppm in +CSA), with one of them with a slight deshielding effect, while the other one showed a relevant up-fielding; different $\Delta\delta_{form}$ were observed in the case of the two hydrogens in -CH_2- signal in α to -SO_3H, suggesting a possible interaction of only one of them with the other molecule. The acid hydrogen of -SO_3H portion showed a relevant shift of its signal with a relevant shielding; this suggests an interaction of this part of the molecule with FS. The chemical shift of acid hydrogens varies very much, and this is certainly due to the presence of an H-

bond between the component of the DES. $\Delta\delta_{form}$ depends for sure on the values of K_f, but, likely, also on other factors, such as the possibly different amount of water in the samples. For this, its $\Delta\delta_{form}$ will not be quantitatively analyzed. In the ammonium FR and FS signals, a deshielding was observed for almost all the peaks: the aromatic hydrogens, the -CH_3 on the chiral centre, the -CH_3 in methanesulfonate counterion; on the contrary, a shielding effect was observed for the hydrogen in the chiral centre. The -$N(CH_3)_3$ signals showed a peculiar effect because they resulted shielded in the case of FS and slightly deshielded in the case of FR. The hydrogen in the chiral centre showed also a sensitive different of $\Delta\delta_{form}$ between the two couples. This could mean a different organization of the molecules in the liquids once interacting with CSA, with FS that could be closer to the negative charge of the counterion (or to the CSA/methanesulfonate couple) compared to the pure ammonium, while it could be more distant in the case of FR. These data suggested that electrostatic and H-bond interactions could occur between HBD and HBA molecules in these systems, but also other ones involving other portions of the molecules such as the hydrogens in -CH_2- signal in α to -SO_3H, the ones of the geminal methyl in CSA, the hydrogens next to the chiral centre in FR and FS. For a simple and fast visualization of these results, in Figure 3 the chemical structures of the DESs +CSA/FR and +CSA/FS DESs are reported, with the relevant hydrogens coloured following a scale based on the intensity of $\Delta\delta_{form}$ passing from the pure components to the DESs. The other peaks of the hydrogens on the CSA ring were not reported for a clearer visualization, because they did not show any significant difference between the two mixtures.

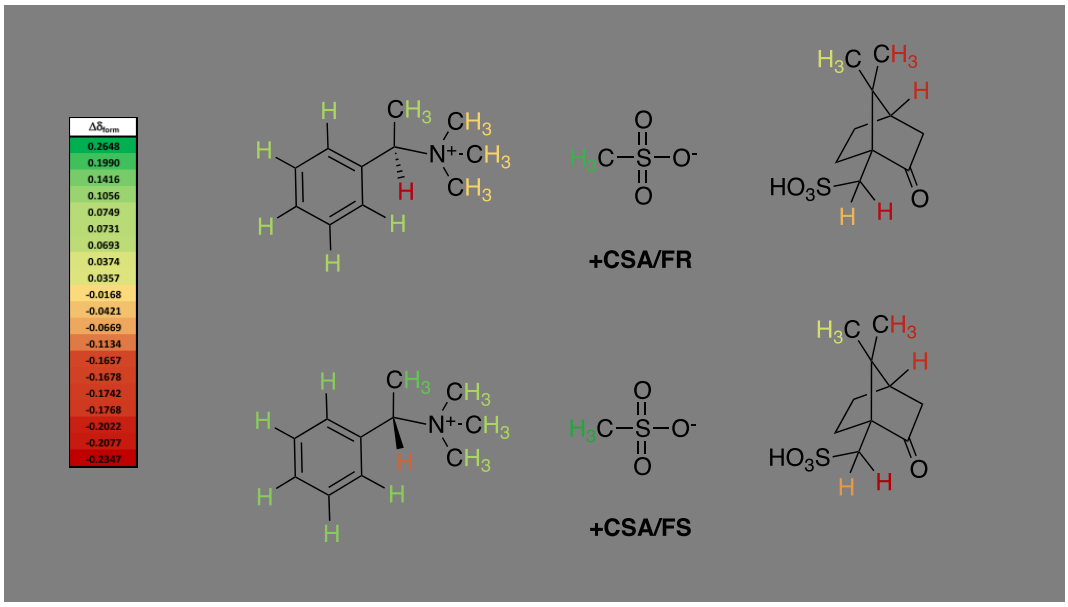

Figure 3: $\Delta\delta_{form}$ = differences (in ppm) of the chemical shifts of the signals of the DESs and the pure components. +CSA/FR (up), +CSA/FS (down). Some peaks of the hydrogens of the CSA ring were not reported for a clearer visualization, because they did not show any significant difference between the two mixtures.

The next step was the comparison between the spectra of the formed DESs; in Figure 4 the stacked spectra of +CSA/FR and +CSA/FS DESs are reported. The $\Delta\delta_{DESs}$ values (differences in ppm between +CSA/FR and +CSA/FS signals) were evaluated.

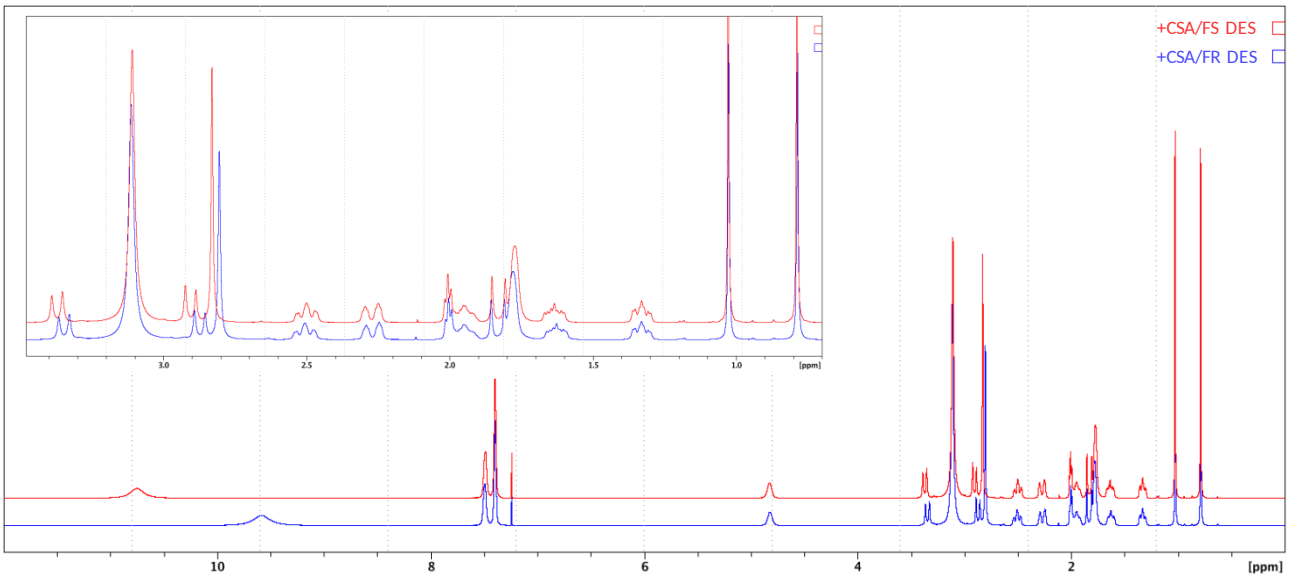

Figure 4: Stacked ^{1}H-NMR spectra of the DESs couples +CSA/FS (red) and +CSA/FR (blue) in $CDCl_3$. Inlet: the same spectra enlarged in the range 0.5-3.5 ppm. All the spectra were calibrated on solvent signal.

The spectra of the two DESs showed differences in the chemical shifts of their peaks; therefore these liquids resulted differently structured. The acid hydrogen of -SO_3H showed a significant shift, that resulted more shielded in the +CSA/FR DES compared to +CSA/FS; this is mostly due to the fact that in the case of +CSA/FR the value of K_f is lower than in the case of +CSA/FS, but, as mentioned before, these signals cannot be analyzed in the same manners of the other ones because of the influence on their chemical shifts of possibly different amounts of water in the mixtures. Other shifts in the signals were observed for specific peaks of CSA and of FR and FS. In the ammonium molecules, +CSA/FR DES showed peaks at higher ppm compared to the ones of +CSA/FS, except for the ones of the hydrogen in the chiral center. The most up-shifted signal between the two liquids was the -CH_3 in the chiral center. In +CSA all the signals were at lower ppm in +CSA/FR compared to +CSA/FS, except for the hydrogen on the tertiary carbon in the ring that resulted at higher ppm in +CSA/FR. In Figure 5 the structures with the hydrogens colored following the $\Delta\delta_{DESs}$ values are reported.

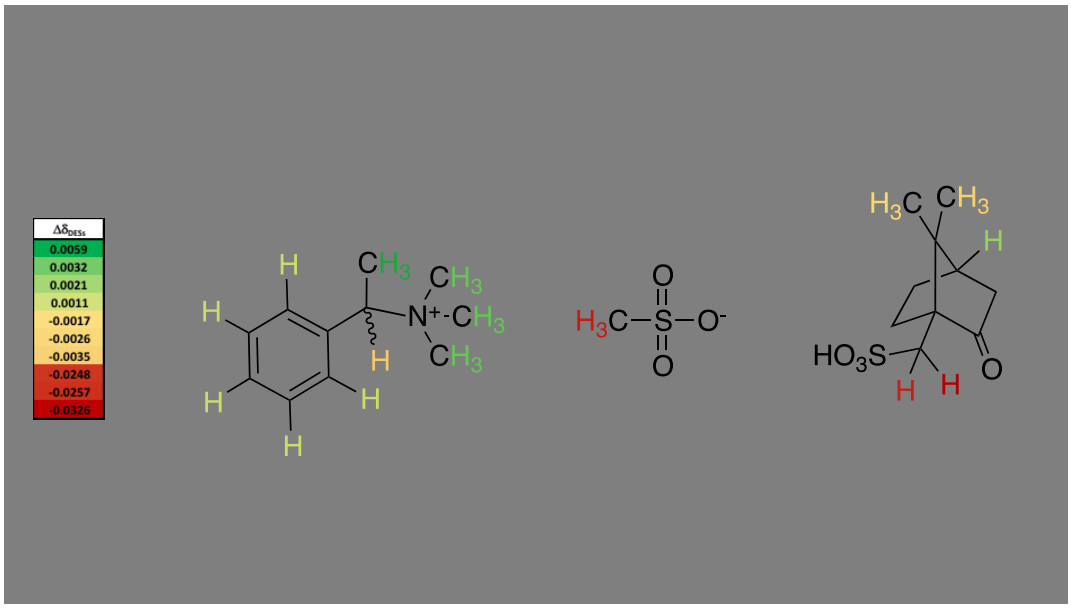

Figure 5: $\Delta\delta_{DESs}$ = differences (in ppm) between the chemical shifts of the signals of +CSA/FR DES and +CSA/FS DES.

The observed differences between the liquids with the same HBD and with the two enantiomers of the HBA, suggested to analyse all the couples used in the addition reaction in which these DESs were used as solvents, following the order used in Table 3 (see supporting info Figure S15, Table S6). Surprisingly, the differences in chemical shifts between the liquid couples ($\Delta\delta_{DESs}$) for the most shifted signals were found to correlate with the differences in the yields obtained using the DESs as solvents in the reaction (Δ_{yields}). Therefore, a correlation between the Δ_{yields} with the $\Delta\delta_{DESs}$ was performed considering all the $\Delta\delta_{DESs}$ of each single peak. The coefficient of determination R^2 was considered here only as an evaluation of the most relevant peaks, because the R^2 values themselves cannot be considered as statistically relevant, since they are derived from a set of only four points (that is the number of different couples of liquids that can be structurally compared). However, these data gave us important information on the role of the portion of the molecules involved in the diastereoisomerically differences between the liquids. All the data are reported in Supporting Information section, Table S7. The most relevant data were observed for three signals: the $\Delta\delta_{DESs}$ values of the two hydrogens of -CH_2- signal in α to -SO_3H and of CH_3- in methanesulfonate counterion. These signals showed the highest R^2 values correlating their differences between the liquids with the Δ_{yields} of the same mixtures (R^2 = 0.97558, 0.97548 and 0.98193 respectively). All the other R^2 values observed for all the others possible combinations were lower, and they spanned from 0.02946 to 0.29263. The interactions between the +CSA and the methanesulfonate counterion, therefore of the portions involved in the H-bond, seemed to determine mostly the diastereoisomerically differences in these liquids. These parts of the molecules could be in turn

affected by the position of the ammonium itself and of the two enantiomers of it. The last step of this work is represented by Density Functional Theory studies (DFT) that helped optimize the geometry of the various adducts.

2.2.4 DFT Studies.

Likely, a complex network of interactions exists between the three components of the adducts, with small differences depending on the chirality of the ammonium cation. In order to shed some light on these differences, the geometry of the various adducts have been optimized by Density Functional Theory (DFT, more details in the Computational Section) at BP86-D3/def-TZVP level.

Firstly, the geometry of the supramolecular anion formed by the methanesulfonate and the +CSA has been optimized. There are three main interactions between the two units (Figure 6): a strong hydrogen bond involving the acid proton (which in this case it is shifted toward the methanesulfonate because of the absence of the cation) and two weaker electrostatic interactions between partially negative oxygen atoms and partially positive -CH-. In particular, the interaction involves only one proton of the -CH_2- signal in α to -SO_3H of +CSA, in agreement with the experimental observations in $\Delta\delta_{form}$ section.

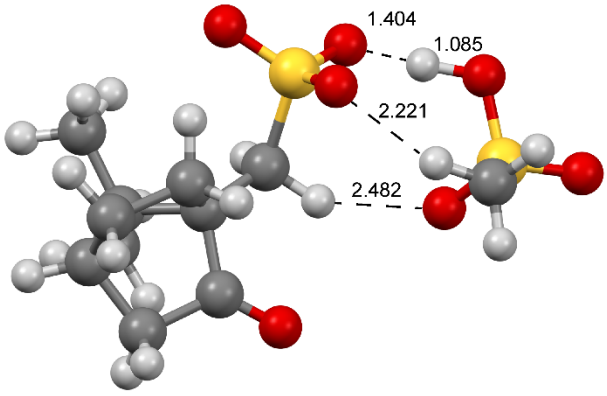

Figure 6: Optimized geometry of the supramolecular-anion methanesulfonate/+CSA (distances in Å).

Including the cation, 4 different structures have been optimized. In fact, the cation can interact with the macro-anion using not only the cationic "head" -$N(CH_3)_3$, but also the -$CH(CH_3)$- moiety that bridges the ammonium and the phenyl groups, through the proton of the CH or the CH_3. Further, the cation has been considered in its two enantiomers, S and R, leading to the four structures S_CH, S_CH_3, R_CH and R_CH_3 (Figure 7).

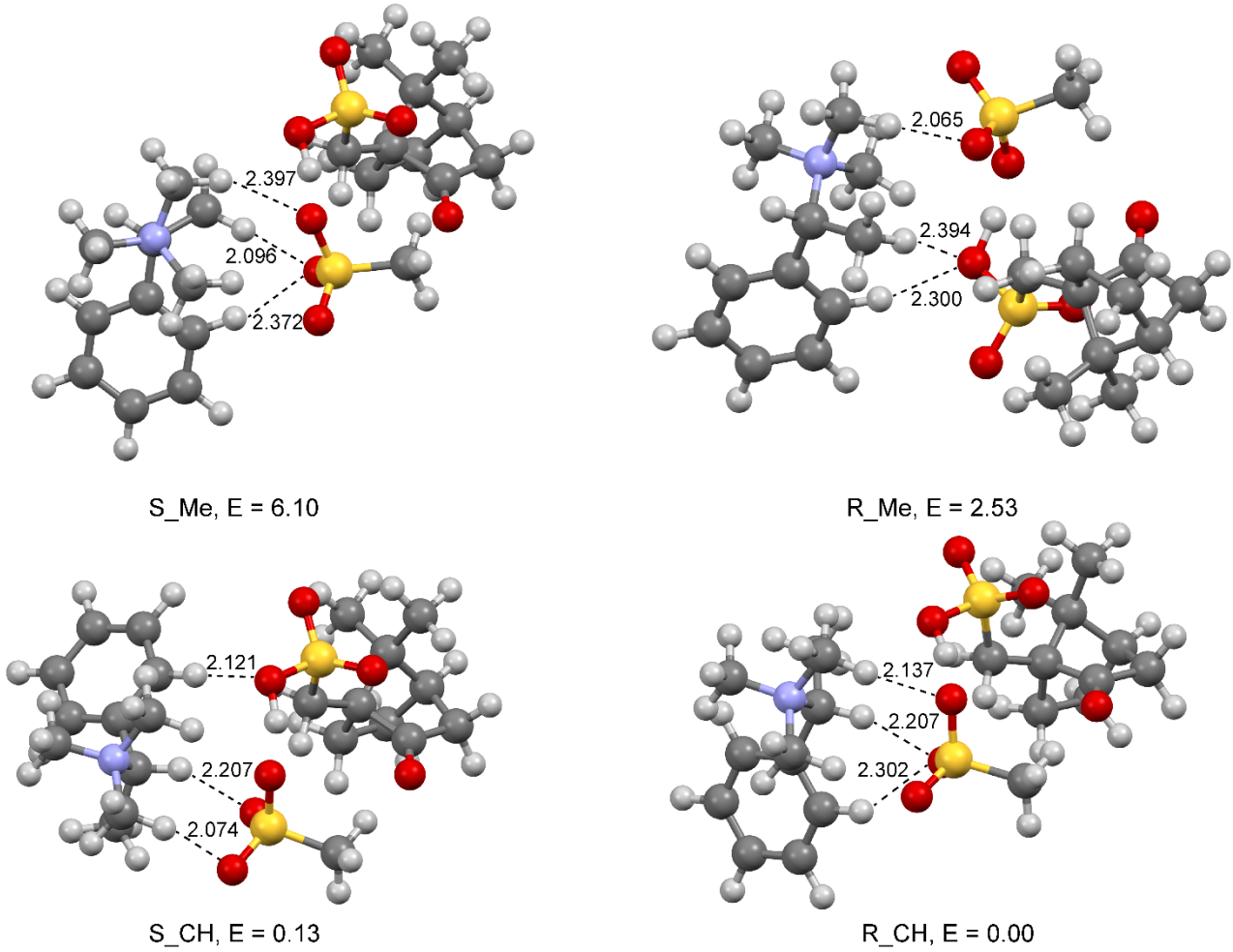

Figure 7: Optimized geometry of different adducts (distances in Å, energies in kcal/mol).

The most stable structures are those using the CH moiety, which decreases the steric hindrance between the +CSA and the cation, with a small difference between the two enantiomers of the cation (as evidenced also in the NMR titrations section). The two supramolecular structures differ in the nature of the interactions: in S_CH, the aromatic proton interacts with the oxygen of +CSA, whereas in R_CH the same proton interacts with one oxygen of the anion. Anyway, the number of simultaneous interactions guarantees the stability and rigidity of both the structures.

Noteworthy, the cation-anion distance is larger in the adduct (2.074 and 2.207 Å for S_CH, 2.137 and 2.207 Å for R_CH) than in the absence of +CSA (2.051 and 2.081 Å in FS and FR), whereas the distance between the methanesulfonate and the +CSA are almost the same in the presence and absence of the cation, except for the acid proton. Indeed, the OH bond distance in the isolated +CSA is 0.978 Å, which is stretched up to 1.404 Å in the supramolecular anion and results to be elongated to 1.063 Å in the S_CH adduct. This is relevant to interpret the decrease of the melting point of these DESs mixtures: the larger distance between the cation and the anion determines a weaker

electrostatic interaction between the molecules, therefore a decrease of the melting point of the mixtures. This effect was determined by the H-interactions between the +CSA and the methanesulfonate that provoked a decrease of the negative charge density in the anion, therefore a weaker interaction with the ammonium cation. The same effect was observed and studied in literature with other DESs mixtures and it is proved to be responsible for the decrease of the melting points of the mixtures.[21,51–53] Moreover, the differences observed between the +CSA/FR and +CSA/FS mixtures were in agreement with the data observed in ^{1}H-NMR titrations and in $\Delta\delta_{DESs}$ analysis, where differences in the portions involved in the electrostatic interactions were observed between the two DESs.

Noteworthy, in the optimized geometry of S_CH and R_CH, the distance between selected protons of the +CSA and those of the cation or the methanesulfonate are around or lower than 3 Å (SO_3CH_2···aromatic CH = 2.611 Å in S_CH, SO_3CH_2···CH_3SO_3 = 3.062 Å in R_CH, SO_3CH_2···CH_3CH = 2.749 Å in R_CH), suggesting the possibility to detect intermolecular Nuclear Overhauser Effects through the ^{1}H NOESY technique. Unfortunately, we were not able to detect such contacts, either at high and low concentration in chloroform. Among the possible explanations, it is possible that in solution the intermolecular distances are longer than in the DFT-optimized geometries, due to the solvent dielectric properties (ε_r of chloroform is 4.81).

The possibility of multiple sites of interactions between +CSA and the methanesulfonate counterion and between the cation and the macro-anion is a relevant factor that must be considered to evaluate the complexity of these liquids and therefore their properties. A chloride counterion, in fact, cannot lead to this structural complexity because of its spherical shape and, even if can lead to multiple interactions, it does not have different sites of interactions with the HBA and/or the HBD molecules as well as the methanesulfonate.

As a further proof of the relevance of methanesulfonate anion portion (and its interaction with +CSA) in the DESs formation, recently we observed peculiar behaviours of the melting points of a novel class of DESs we realized.[12] These mixtures were based on the interactions of molecules that are similar to the ones of this work: +CSA as HBD and sulfobetaines as HBAs. Even if they derived from widely differently structured sulfobetaines (aliphatic, aromatic and amphiphilic ones), these mixtures showed melting points that were very similar in all the obtained liquids (close to room temperature) and also similar to the ones of these novel chiral DESs. This suggested that the +CSA and the alkyl-sulfonate portions are relevant in determining the lowering of the melting points of these mixtures.

3. EXPERIMENTAL

3.1 General

(1R)-(-)-10-camphorsulfonic acid, (1S)-(+)-10-camphorsulfonic, methyl methanesulfonate, chalcone, indole, (R)-(+)-1-phenylethylamine, (S)-(-)-1-phenylethylamine (all the purities > 98%), d-chloroform and all the solvents were purchased from Sigma-Aldrich, Alfa Aesar and Merck and were used without further purification. (1R)-(-)-10-Camphorsulfonic acid, (1S)-(+)-10-Camphorsulfonic acid were used after drying under vacuum over P_2O_5. All the yields are reported as isolated yields. The freezing points of the DESs were determined cooling the mixtures in an ice bath and determining the freezing temperature with a thermometer.

3.2 DESs preparation

- Synthesis of (R)-*N*,*N*,*N*-trimethyl-(1-phenylethyl)ammonium methanesulfonate: (R)-(+)-1-phenylethylamine (10 g, 1 eq) was dissolved in CH_3CN in presence of K_2CO_3 (23 g, 2 eq). Methyl-methanesulfonate (27.3 g, 3 eq) was added dropwise to the magnetically stirred solution at room temperature. After 8 hours, the mixture was filtered and dried under vacuum. The product was re-crystallized in ethyl acetate to give white crystals (Yield = 86%), m.p. = 166-168°C. ^{1}H-NMR (400MHz, $CDCl_3$) δ = 7.46 – 7.25 (m, 5H); 4.95 – 4.90 (m, 1H); 3.04 (s, 9H); 2.54 (s, 3H); 1.65 – 1.63 (d, 3H). ^{13}C-NMR (101 MHz, $CDCl_3$) δ = 132.6; 130.1; 128.7; 72.6; 50.4; 39.4; 14.6.

- Synthesis of (S)-*N*,*N*,*N*-trimethyl-(1-phenylethyl)ammonium methanesulfonate: the procedure was identical to the one of the R-ammonium salt, using (S)-(-)-1-phenylethylamine. (Yield = 82%), m.p. = 166-168°C. ^{1}H-NMR (400MHz, $CDCl_3$) δ = 7.46 – 7.25 (m, 5H); 4.95 – 4.90 (m, 1H); 3.04 (s, 9H); 2.54 (s, 3H); 1.65 – 1.63 (d, 3H). ^{13}C-NMR (101 MHz, $CDCl_3$) δ = 132.6; 130.1; 128.7; 72.6; 50.4; 39.4; 14.6.

- DESs preparation: The HBD solid molecule was weighed in a vial or in a flask with the solid HBA molecule at the proper molar ratio (1:1). The two solids were mixed with a vortex mixer for few minutes and then heated in an oil bath (or in an oven) at 70°C until a homogeneous liquid was formed (typically 1 to 3 hours).

3.3 Michael-type Friedel-Crafts probe reaction addition procedure

In a typical experiment, chalcone (50 mg, 1 eq) was weighed in a vial with a small excess of indole (30 mg, 1.1 eq) and the DES (0.5 g). The mixture was stirred at 40°C for 30 minutes in an oil bath.

Then the mixture was quantitatively transferred in a separating funnel with water and ethyl acetate, and then extracted three times with ethyl acetate. The organic phases were dried under Na_2SO_4. The products were purified via column chromatography with ethyl acetate:petroleum ether (1:5) as eluent, giving a red solid (m.p. = 142-144°C). The most relevant reactions were repeated three times, giving the same yields of weighted product (±2%). ^{1}H-NMR (400 MHz, $CDCl_3$) δ = 7.97 (brs, 1H); 7.92–7.90 (m, 2H); 7.52 (m, 1H); 7.43–7.40 (m, 3H); 7.34 (d, 2H); 7.29 (m, 1H); 7.23 (m, 2H); 7.16–7.10 (m, 2H); 7.00 (m, 1H); 6.96 (m, 1H); 5.05 (m, 1H); 3.80 (m, 1H); 3.71 (m, 1H). ^{13}C-NMR (100 MHz, $CDCl_3$) δ = 198.6, 144.2, 137.2, 136.6, 133.0, 128.6, 128.4, 128.1, 127.8, 126.6, 126.3, 122.1, 121.4, 119.6, 119.4, 119.3, 111.1, 45.2, 38.3.

3.4 Enantiomeric excess determination

For all the enantioselective chromatography analyses, a Chiralcel OD-H column (250 mm x 4.6 mm I.D) from Chiral Technologies (West Chester, PA, USA) was used.[54] This chiral stationary phase carries a cellulose *tris*(3,5-dimethylphenylcarbamate) chiral selector adsorbed onto a 5 μm silica gel. All the runs were carried out with a (*n*-hexane/2-propanol 75:25 (v/v) eluent system flowed at a 0.5 mL/min. Column temperature was fixed a 25 °C through a Grace (Sedriano, Italy) heater/chiller (Model 7956R) thermostat. Analytical grade n-hexane and 2-propanol were purchased from Sigma-Aldrich. The compound 1,3,5-tri-*tert*-butylbenzene was used as the unretained marker and purchased from Sigma-Aldrich. The employed mobile phase was degassed with 10 min sonication before use. Compounds to be injected were solubilized in the selected mobile phase and analyzed at the approximate concentration of 0.5-1.0 mg/mL. Before use, the column was conditioned with the selected mobile phase at a 0.5 mL/min flow rate for at least 40 min. The HPLC analyses were performed on a Shimadzu (Kyoto, Japan) LC-20A Prominence, equipped with a CBM-20A communication bus module, two LC-20AD dual piston pumps, a SPD-M20A photodiode array detector, and a Rheodyne 7725i injector (Rheodyne Inc., Cotati, CA, USA) with a 100 μL stainless steel loop. With the above experimental conditions all enantiomer pairs under investigation were base-line separated (resolution factor values higher than 1.5, Table 1). An exemplary chromatogram for the product obtained in -CSA/FR is shown in Supporting Information section (Figure S2). The chromatographic parameters were calculated according to the German Pharmacopeia (DAB). The retention factor (*k*) values were computed by taking the retention time (t_R) at the peak maximum. Enantioseparation factor (α) and resolution factor (R_S) were computed from the following Eqs.:

$$\alpha = \frac{k_2}{k_1}$$

$$R_S = 1.18 \frac{t_R - t_{Rp}}{W_{0.5} + Wp_{0.5}}$$

where k_1 is the retention factor of the first eluted enantiomer, k_2 is the retention factor of the second eluted enantiomer, $W_{0.5}$ is the width of the peak at the position of 50% peak height, $Wp_{0.5}$ is the width of the peak at the position of previous 50% peak height and t_{Rp} is the retention time of the first eluted peak within each enantiomer couple.

3.5 NMR measurements

^{1}H-NMR spectra were measured at 298 K on a Bruker DRX Avance 400 spectrometer equipped with a BBFO probe and on a Bruker Avance III HD. All the spectra were calibrated on solvents signals.

3.6 PGSE NMR measurements

^{1}H PGSE NMR[55–58] measurements were performed by using the double-stimulated echo sequence with longitudinal eddy current delay at 298 K without spinning. The dependence of the resonance intensity (I) on a constant waiting time and on a varied gradient strength G is described by the following equation:

$$ln\frac{I}{I_0} = (\gamma\delta)^2 D_t \left(\Delta - \frac{\delta}{3}\right) G^2$$

where I is the intensity of the observed spin echo, I_0 the intensity of the spin echo in the absence of gradient, D_t the self-diffusion coefficient, Δ the delay between the midpoints of the gradients (0.2 s), δ the length of the gradient pulse (4 ms), and γ the magnetogyric ratio. The shape of the gradients was rectangular, and their strength G was varied during the experiments.

The self-diffusion coefficient D_t, was estimated by evaluating the proportionality constant for a sample of HDO (5%) in D_2O (known diffusion coefficients in the range 274–318 K[59]) under the exact same conditions as the sample of interest. The solvent or TMS was taken as internal standard. The hydrodynamic volume of the species has been calculated from the experimental value of D_t through the procedure previously described.[48] In supporting information section the Linear trends of $\ln(I/I_0)$ *vs*. G^2 are reported (Figures S3-S12).

3.7 Computational details

All the geometries were optimized with ORCA 3.0.3,[60] using the BP86 functional[61,62] in conjunction with the def2-TZVP basis set. The dispersion corrections were taken into account using the Grimme D3-parametrized XC functionals.[63] No substantial differences have been noted computing the final energies using the B3-LYP functional[64] and the same basis set. All the optimized geometries resulted to be local energy minima (no negative vibrations). All the data are reported in Supporting Information section (Table S8).

4. CONCLUSIONS

Novel chiral Deep Eutectic Solvents were realized and studied. The chiral HBD and HBA molecules are common, relatively cheap and commercially available (+CSA and -CSA as HBD) or easily one-step synthesized from commercially available compounds (FR and FS as HBA). All the combinations of the two enantiomers (and also the racemates) were used to obtain liquids at room temperature. These systems revealed specific properties depending on the enantiomer used as HBD or HBA, revealing to be high-structured liquids.

These liquids were used as reaction media / chiral organocatalysts / acid catalysts in a Friedel-Craft Michael-type probe addition. Different yields and different e.e. were observed with the different combinations of the enantiomers of the HBD and HBA molecules. The e.e. were low, but comparable to the ones observed in literature with the use of toluene, dichloromethane or CH_3CN solvents with the addition of +CSA. The different yields observed in the liquids suggested diastereoisomerical differences among these mixtures; therefore +CSA/FR and +CSA/FS DESs were structurally analyzed with different NMR techniques and with Density Functional Theory geometry optimization.

^{1}H Pulsed Field gradient Spin Echo (PGSE) NMR studies showed these systems as clusters of about 4 couples of HBD-HBA at the concentration of 0.1 mg/mL in $CDCl_3$, so all the NMR measures were performed at these concentrations. The ^{1}H-NMR titrations revealed different constants of association between the HBD and HBA molecules in the two mixtures +CSA/FR and +CSA/FS. ^{1}H NMR spectra analysis confirmed these differences in terms of $\Delta\delta_{form}$ (δ_{DES} - $\delta_{pure\ compounds}$) and in terms of $\Delta\delta_{DESs}$ (differences in ppm between +CSA/FR and +CSA/FS signals). These analyses indicated that the portions of the molecules involved in the H-bonds and in the electrostatic interactions (methanesulfonate counterion, $-SO_3H$, $-CH_2-$ in α at $-SO_3H$) were the most different between the

two DESs. Surprisingly, the differences in the yields of the probe reaction in the liquids correlate with the $\Delta\delta_{DESs}$ of the most different peaks.

Finally, Density Functional Theory geometry optimization showed the relevance of the role of the methanesulfonate counterion in order to explain and interpret the complexity of the structures. The multiple-site interactions that can occur between the +CSA and the counterion led to a structured supramolecular-anion that can interact differently with the two enantiomers of the ammonium HBA molecule.

These novel Chiral Deep Eutectic Solvents revealed to be promising high-structured liquids for enantioselective Brønsted acid catalysed reaction.

CONFLICT OF INTEREST

The authors declare no conflict of interest.

ACKNOWLEDGEMENT

This research did not receive any specific grant from funding agencies in the public, commercial, or not-for-profit sectors.

FUNDING

This research did not receive any specific grant from funding agencies in the public, commercial, or not-for-profit sectors.

REFERENCES

[1] K.N. Marsh, J.A. Boxall, R. Lichtenthaler, Room temperature ionic liquids and their mixtures—a review, Fluid Phase Equilib. 219 (2004) 93–98.

[2] R.A. Sheldon, The E factor 25 years on: the rise of green chemistry and sustainability, Green Chem. 19 (2017) 18–43.

[3] T. Welton, Room-temperature ionic liquids. Solvents for synthesis and catalysis, Chem. Rev. 99 (1999) 2071–2084.

[4] R.D. Rogers, K.R. Seddon, Ionic liquids--solvents of the future?, Science (80-.). 302 (2003) 792–793.

[5] J.G. Huddleston, H.D. Willauer, R.P. Swatloski, A.E. Visser, R.D. Rogers, Room temperature ionic liquids as novel media for “clean”liquid–liquid extraction, Chem. Commun. (1998) 1765–1766.

[6] F. Cardellini, L. Brinchi, R. Germani, M. Tiecco, Convenient Esterification of Carboxylic Acids by SN2 Reaction Promoted by a Protic Ionic Liquid System Formed in Situ, in Solvent-Free Conditions, Synth. Commun. 44 (2014) 3248–3256.

[7] T.P.T. Pham, C.-W. Cho, Y.-S. Yun, Environmental fate and toxicity of ionic liquids: a review, Water Res. 44 (2010) 352–372.

[8] D. Zhao, Y. Liao, Z. Zhang, Toxicity of ionic liquids, Clean–soil, Air, Water. 35 (2007) 42–48.

[9] A. Romero, A. Santos, J. Tojo, A. Rodriguez, Toxicity and biodegradability of imidazolium ionic liquids, J. Hazard. Mater. 151 (2008) 268–273.

[10] E.L. Smith, A.P. Abbott, K.S. Ryder, Deep eutectic solvents (DESs) and their applications, Chem. Rev. 114 (2014) 11060–11082.

[11] A.P. Abbott, D. Boothby, G. Capper, D.L. Davies, R.K. Rasheed, Deep eutectic solvents formed between choline chloride and carboxylic acids: versatile alternatives to ionic liquids, J. Am. Chem. Soc. 126 (2004) 9142–9147.

[12] F. Cardellini, R. Germani, G. Cardinali, L. Corte, L. Roscini, N. Spreti, M. Tiecco, Room temperature deep eutectic solvents of (1S)-(+)-10-camphorsulfonic acid and sulfobetaines: Hydrogen bond-based mixtures with low ionicity and structure-dependent toxicity, RSC Adv. 5 (2015) 31772–31786.

[13] Q. Zhang, K.D.O. Vigier, S. Royer, F. Jérôme, Deep eutectic solvents: syntheses, properties and applications, Chem. Soc. Rev. 41 (2012) 7108–7146.

[14] H. Zhao, G.A. Baker, S. Holmes, Protease activation in glycerol-based deep eutectic solvents, J. Mol. Catal. B Enzym. 72 (2011) 163–167.

[15] R. Germani, M. Orlandini, M. Tiecco, T. Del Giacco, Novel low viscous, green and amphiphilic N-oxides/phenylacetic acid based Deep Eutectic Solvents, J. Mol. Liq. 240 (2017) 233–239. doi:10.1016/j.molliq.2017.05.084.

[16] Z. Maugeri, P.D. de María, Novel choline-chloride-based deep-eutectic-solvents with renewable hydrogen bond donors: levulinic acid and sugar-based polyols, Rsc Adv. 2 (2012) 421–425.

[17] A. Paiva, R. Craveiro, I. Aroso, M. Martins, R.L. Reis, A.R.C. Duarte, Natural deep eutectic solvents–solvents for the 21st century, ACS Sustain. Chem. Eng. 2 (2014) 1063–1071.

[18] Y. Dai, J. van Spronsen, G.-J. Witkamp, R. Verpoorte, Y.H. Choi, Natural deep eutectic solvents as new potential media for green technology, Anal. Chim. Acta. 766 (2013) 61–68.

[19] Y.H. Choi, J. van Spronsen, Y. Dai, M. Verberne, F. Hollmann, I.W.C.E. Arends, G.-J. Witkamp, R. Verpoorte, Are natural deep eutectic solvents the missing link in understanding cellular metabolism and physiology?, Plant Physiol. 156 (2011) 1701–1705.

[20] H.G. Morrison, C.C. Sun, S. Neervannan, Characterization of thermal behavior of deep eutectic solvents and their potential as drug solubilization vehicles, Int. J. Pharm. 378 (2009) 136–139.

[21] A.P. Abbott, G. Capper, D.L. Davies, R.K. Rasheed, V. Tambyrajah, Novel solvent properties of choline chloride/urea mixtures, Chem. Commun. (2003) 70–71.

[22] M. Hayyan, M.A. Hashim, M.A. Al-Saadi, A. Hayyan, I.M. AlNashef, M.E.S. Mirghani, Assessment of cytotoxicity and toxicity for phosphonium-based deep eutectic solvents, Chemosphere. 93 (2013) 455–459.

[23] K. Radošević, M.C. Bubalo, V.G. Srček, D. Grgas, T.L. Dragičević, I.R. Redovniković, Evaluation of toxicity and biodegradability of choline chloride based deep eutectic solvents, Ecotoxicol. Environ. Saf. 112 (2015) 46–53.

[24] M. Hayyan, M.A. Hashim, A. Hayyan, M.A. Al-Saadi, I.M. AlNashef, M.E.S. Mirghani, O.K. Saheed, Are deep eutectic solvents benign or toxic?, Chemosphere. 90 (2013) 2193–2195.

[25] F. Cardellini, M. Tiecco, R. Germani, G. Cardinali, L. Corte, L. Roscini, N. Spreti, Novel zwitterionic deep eutectic solvents from trimethylglycine and carboxylic acids: Characterization of their properties and their toxicity, RSC Adv. 4 (2014) 55990–56002.

[26] J. Chen, Q. Wang, M. Liu, L. Zhang, The effect of deep eutectic solvent on the pharmacokinetics of salvianolic acid B in rats and its acute toxicity test, J. Chromatogr. B. 1063 (2017) 60–66.

[27] A.P. Abbott, G. Capper, K.J. McKenzie, K.S. Ryder, Electrodeposition of zinc–tin alloys from deep eutectic solvents based on choline chloride, J. Electroanal. Chem. 599 (2007) 288–294.

[28] H. Liao, Y. Jiang, Z. Zhou, S. Chen, S. Sun, Shape-controlled synthesis of gold nanoparticles in deep eutectic solvents for studies of structure–functionality relationships in electrocatalysis, Angew. Chemie. 120 (2008) 9240–9243.

[29] C. Li, D. Li, S. Zou, Z. Li, J. Yin, A. Wang, Y. Cui, Z. Yao, Q. Zhao, Extraction desulfurization

process of fuels with ammonium-based deep eutectic solvents, Green Chem. 15 (2013) 2793–2799.

[30] D.A. Alonso, A. Baeza, R. Chinchilla, G. Guillena, I.M. Pastor, D.J. Ramón, Deep eutectic solvents: The organic reaction medium of the century, European J. Org. Chem. 2016 (2016) 612–632.

[31] M. Tiecco, R. Germani, F. Cardellini, Carbon-carbon bond formation in acid deep eutectic solvent: Chalcones synthesis: Via Claisen-Schmidt reaction, RSC Adv. 6 (2016) 43740–43747.

[32] P.D. de María, Z. Maugeri, Ionic liquids in biotransformations: from proof-of-concept to emerging deep-eutectic-solvents, Curr. Opin. Chem. Biol. 15 (2011) 220–225.

[33] D. Lindberg, M. de la Fuente Revenga, M. Widersten, Deep eutectic solvents (DESs) are viable cosolvents for enzyme-catalyzed epoxide hydrolysis, J. Biotechnol. 147 (2010) 169–171.

[34] D.R. Ñiguez, G. Guillena, D.A. Alonso, Chiral 2-Aminobenzimidazoles in deep eutectic mixtures: recyclable organocatalysts for the enantioselective Michael addition of 1, 3-dicarbonyl compounds to β-nitroalkenes, ACS Sustain. Chem. Eng. 5 (2017) 10649–10656. doi:10.1021/acssuschemeng.7b02613.

[35] R. Martínez, L. Berbegal, G. Guillena, D.J. Ramón, Bio-renewable enantioselective aldol reaction in natural deep eutectic solvents, Green Chem. 18 (2016) 1724–1730.

[36] E. Massolo, S. Palmieri, M. Benaglia, V. Capriati, F.M. Perna, Stereoselective organocatalysed reactions in deep eutectic solvents: highly tunable and biorenewable reaction media for sustainable organic synthesis, Green Chem. 18 (2016) 792–797.

[37] C. Baudequin, D. Brégeon, J. Levillain, F. Guillen, J.-C. Plaquevent, A.-C. Gaumont, Chiral ionic liquids, a renewal for the chemistry of chiral solvents? Design, synthesis and applications for chiral recognition and asymmetric synthesis, Tetrahedron: Asymmetry. 16 (2005) 3921–3945.

[38] P. Wasserscheid, A. Bösmann, C. Bolm, Synthesis and properties of ionic liquids derived from the “chiral pool,” Chem. Commun. (2002) 200–201.

[39] S. Luo, X. Mi, L. Zhang, S. Liu, H. Xu, J. Cheng, Functionalized chiral ionic liquids as highly efficient asymmetric organocatalysts for Michael addition to nitroolefins, Angew. Chemie Int. Ed. 45 (2006) 3093–3097.

[40] C. Baudequin, J. Baudoux, J. Levillain, D. Cahard, A.-C. Gaumont, J.-C. Plaquevent, Ionic liquids and chirality: opportunities and challenges, Tetrahedron: Asymmetry. 14 (2003)

3081–3093.

[41] J. Ding, D.W. Armstrong, Chiral ionic liquids: synthesis and applications, Chirality. 17 (2005) 281–292.

[42] K. Bica, P. Gaertner, Applications of chiral ionic liquids, European J. Org. Chem. 2008 (2008) 3235–3250.

[43] M. Orlandi, J.A.S. Coelho, M.J. Hilton, F.D. Toste, M.S. Sigman, Parametrization of Non-covalent Interactions for Transition State Interrogation Applied to Asymmetric Catalysis, J. Am. Chem. Soc. (2017).

[44] F.D. Toste, M.S. Sigman, S.J. Miller, Pursuit of Noncovalent Interactions for Strategic Site-Selective Catalysis, Acc. Chem. Res. 50 (2017) 609–615.

[45] V. De Santi, F. Cardellini, L. Brinchi, R. Germani, Novel Brønsted acidic deep eutectic solvent as reaction media for esterification of carboxylic acid with alcohols, Tetrahedron Lett. 53 (2012) 5151–5155.

[46] W. Zhou, L. Xu, L. Li, L. Yang, C. Xia, Enantioselective Michael-Type Friedel–Crafts Reactions of Indoles to Enones Catalyzed by a Chiral Camphor-Based Brønsted Acid, European J. Org. Chem. 2006 (2006) 5225–5227.

[47] E.O. Stejskal, J.E. Tanner, Spin Diffusion Measurements: Spin Echoes in the Presence of a Time-Dependent Field Gradient, J. Chem. Phys. 42 (1965) 288–292. doi:10.1063/1.1695690.

[48] A. Macchioni, G. Ciancaleoni, C. Zuccaccia, D. Zuccaccia, Determining accurate molecular sizes in solution through NMR diffusion spectroscopy, Chem. Soc. Rev. 37 (2008) 479–489. doi:10.1039/B615067P.

[49] L. Rocchigiani, G. Bellachioma, G. Ciancaleoni, S. Crocchianti, A. Laganà, C. Zuccaccia, D. Zuccaccia, A. Macchioni, Anion-Dependent Tendency of Di-Long-Chain Quaternary Ammonium Salts to Form Ion Quadruples and Higher Aggregates in Benzene, ChemPhysChem. 11 (2010) 3243–3254. doi:10.1002/CPHC.201000530.

[50] P. Thordarson, Determining association constants from titration experiments in supramolecular chemistry, Chem. Soc. Rev. 40 (2011) 1305–1323. doi:10.1039/C0CS00062K.

[51] C.R. Ashworth, R.P. Matthews, T. Welton, P.A. Hunt, Doubly ionic hydrogen bond interactions within the choline chloride–urea deep eutectic solvent, Phys. Chem. Chem. Phys. 18 (2016) 18145–18160.

[52] R. Stefanovic, M. Ludwig, G.B. Webber, R. Atkin, A.J. Page, Nanostructure, hydrogen bonding and rheology in choline chloride deep eutectic solvents as a function of the

hydrogen bond donor, Phys. Chem. Chem. Phys. 19 (2017) 3297–3306.

[53] A. Pandey, D. Dhingra, S. Pandey, Hydrogen Bond Donor/Acceptor Cosolvent-Modified Choline Chloride-Based Deep Eutectic Solvents, J. Phys. Chem. B. 121 (2017) 4202–4212.

[54] B. Natalini, R. Sardella, S. Massari, F. Ianni, O. Tabarrini, V. Cecchetti, Synthesis and chromatographic enantioresolution of anti-HIV quinolone derivatives, Talanta. 85 (2011) 1392–1397.

[55] N.M. Alexej Jerschow, Suppression of Convection Artifacts in Stimulated-Echo Diffusion Experiemnts. Double-Stimulated-Echo Experiments, J. Magn. Reson. 375 (1997) 372–375. doi:10.1006/jmre.1997.1123.

[56] J.P. Fackler, L. Falvello, Techniques in inorganic chemistry, CRC Press/Taylor & Francis, 2011.

[57] G. Ciancaleoni, Characterization of Halogen Bonded Adducts in Solution by Advanced NMR Techniques, Magnetochemistry. 3 (2017) 30. doi:10.3390/magnetochemistry3040030.

[58] P.S. Pregosin, Applications of NMR diffusion methods with emphasis on ion pairing in inorganic chemistry: a mini-review, Magn. Reson. Chem. 55 (2017) 405–413. doi:10.1002/mrc.4394.

[59] R. Mills, Self-diffusion in normal and heavy water in the range 1-45.deg., J. Phys. Chem. 77 (1973) 685–688. doi:10.1021/j100624a025.

[60] F. Neese, The ORCA program system, Wiley Interdiscip. Rev. Comput. Mol. Sci. 2 (2012) 73–78. doi:10.1002/wcms.81.

[61] A.D. Becke, Density-functional exchange-energy approximation with correct asymptotic behavior, Phys. Rev. A. 38 (1988) 3098–3100. doi:10.1103/PhysRevA.38.3098.

[62] J.P. Perdew, Density-functional approximation for the correlation energy of the inhomogeneous electron gas, Phys. Rev. B. 33 (1986) 8822–8824. doi:10.1103/PhysRevB.33.8822.

[63] S. Grimme, J. Antony, S. Ehrlich, H. Krieg, A consistent and accurate ab initio parametrization of density functional dispersion correction (DFT-D) for the 94 elements H-Pu, J. Chem. Phys. 132 (2010) 154104. doi:10.1063/1.3382344.

[64] C. Lee, W. Yang, R.G. Parr, Development of the Colle-Salvetti correlation-energy formula into a functional of the electron density, Phys. Rev. B. 37 (1988) 785–789. doi:10.1103/PhysRevB.37.785.

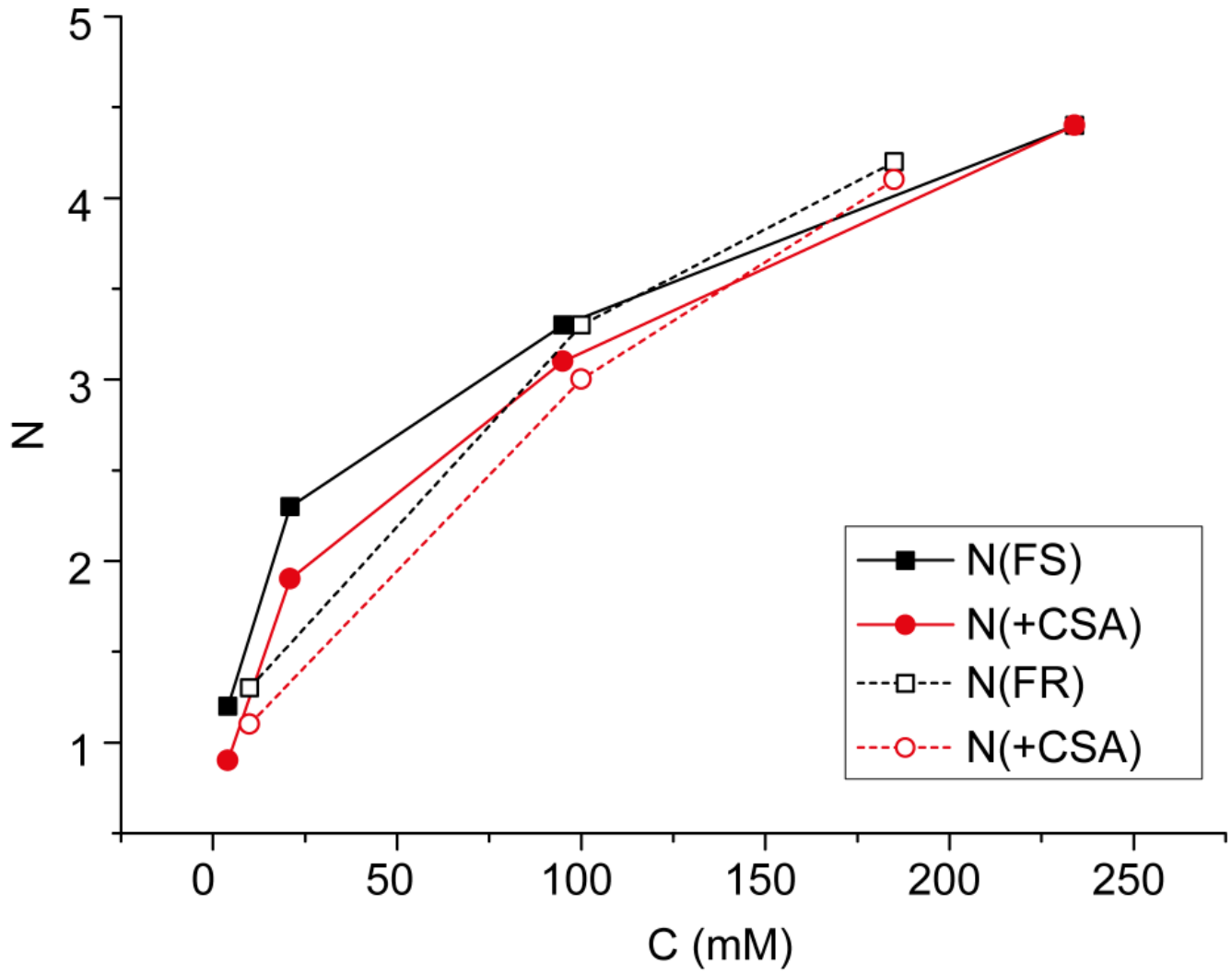

Figure 1: Trend of the aggregation numbers for +CSA/FS (filled symbols) and +CSA/FR (empty symbols).

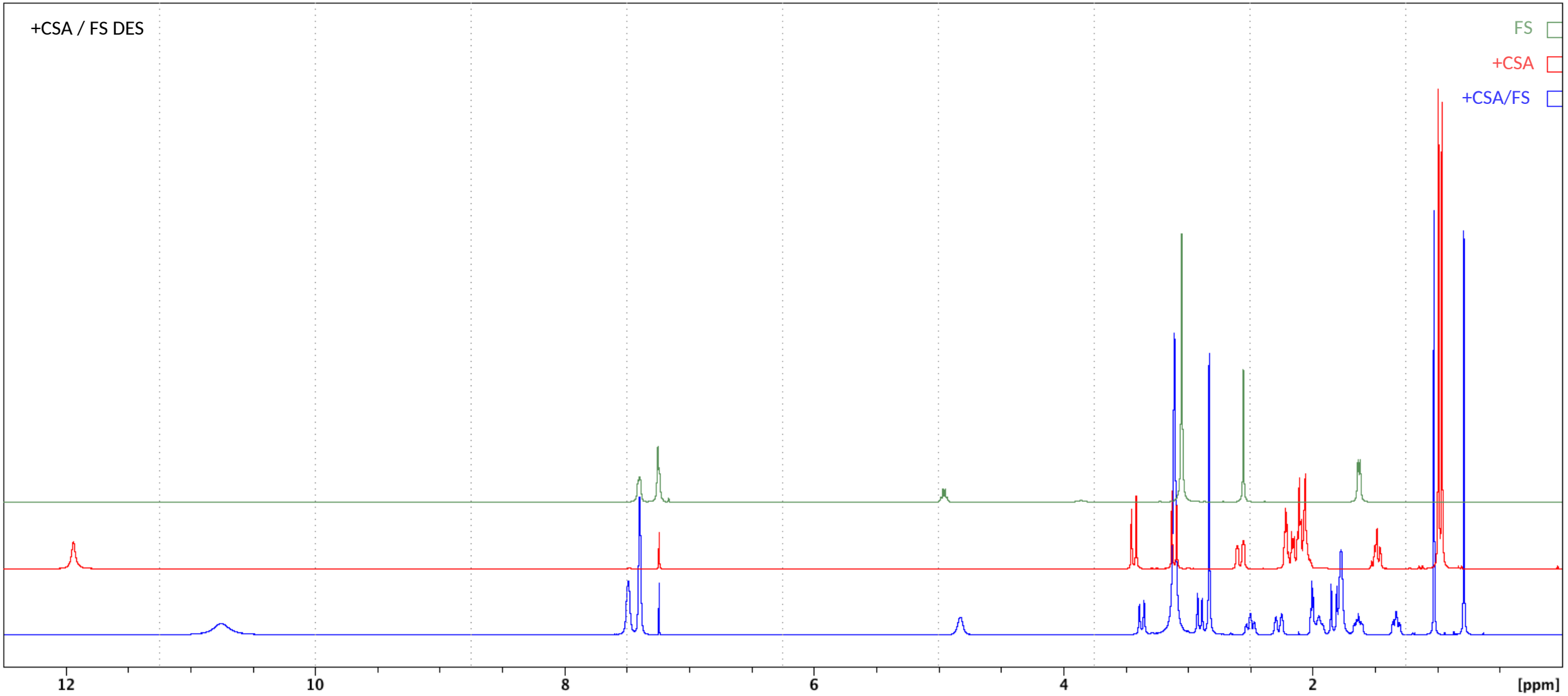

Figure 2: Stacked ^{1}H-NMR spectra in $CDCl_3$ of FS (green), +CSA (red) and the +CSA/FS DES (blue) in $CDCl_3$. All the spectra were calibrated on the solvent signal.

$\Delta\delta_{form}$
0.2648
0.1990
0.1416
0.1056
0.0749
0.0731
0.0693
0.0374
0.0357
-0.0168
-0.0421
-0.0669
-0.1134
-0.1657
-0.1678
-0.1742
-0.1768
-0.2022
-0.2077
-0.2347

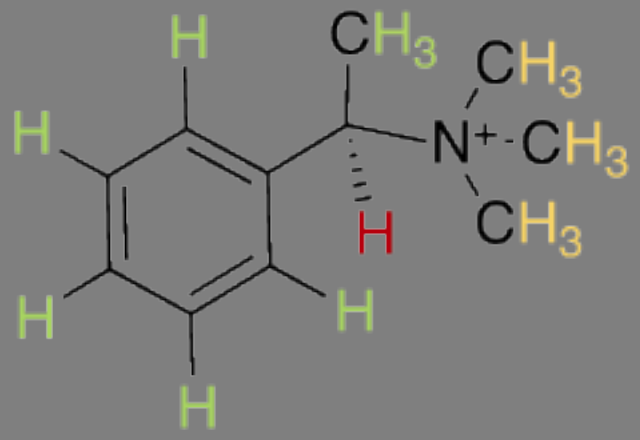

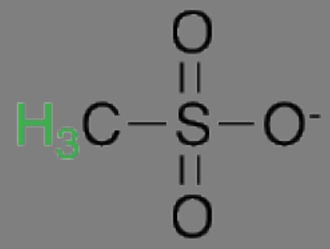

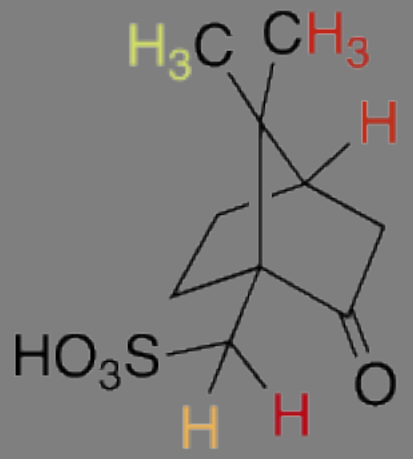

+CSA/FR

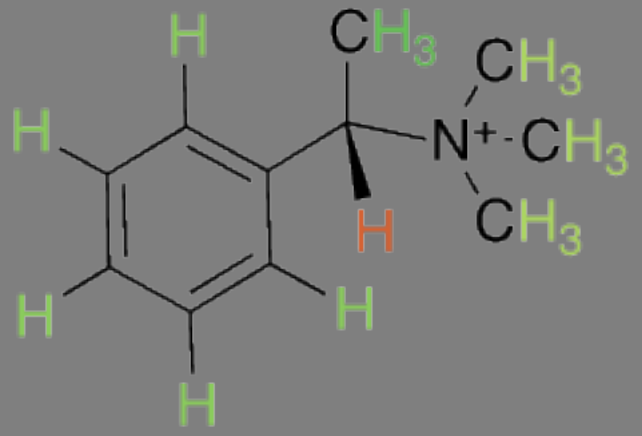

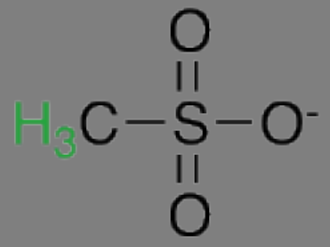

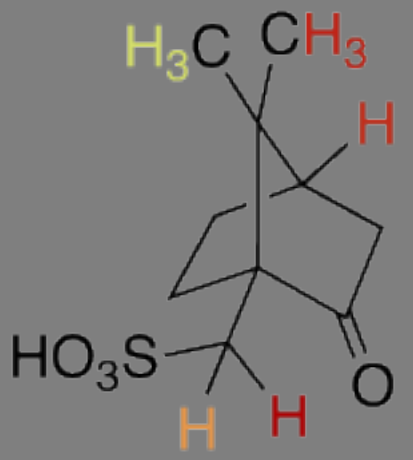

+CSA/FS

Figure 3: $\Delta\delta_{form}$ = differences (in ppm) of the chemical shifts of the signals of the DESs and the pure components. +CSA/FR (up), +CSA/FS (down). Some peaks of the hydrogens of the CSA ring were not reported for a clearer visualization, because they did not show any significant difference between the two mixtures.

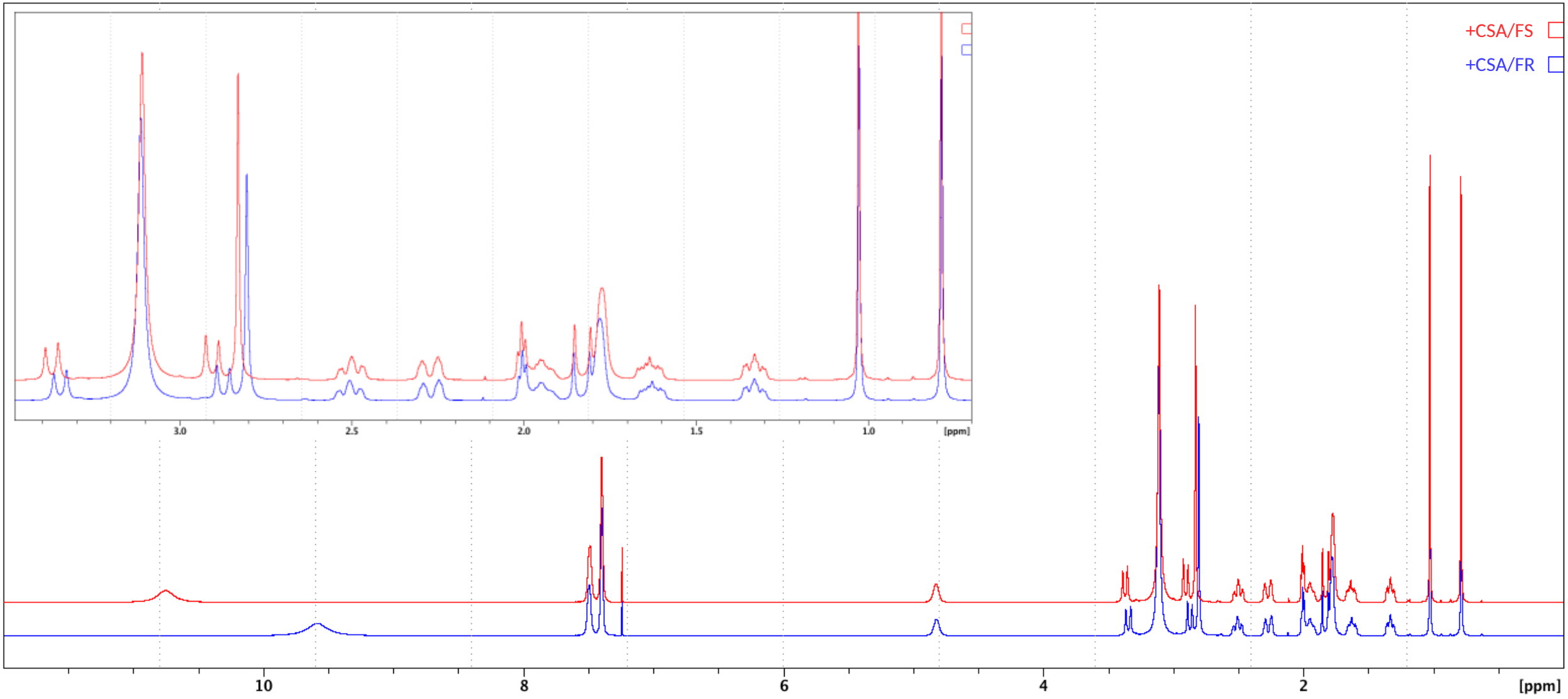

Figure 4: Stacked ^{1}H-NMR spectra of the DESs couples +CSA/FS (red) and +CSA/FR (blue) in $CDCl_3$. Inlet: the same spectra enlarged in the range 0.5-3.5 ppm. All the spectra were calibrated on solvent signal.

$\Delta\delta_{DESs}$
0.0059
0.0032
0.0021
0.0011
-0.0017
-0.0026
-0.0035
-0.0248
-0.0257
-0.0326

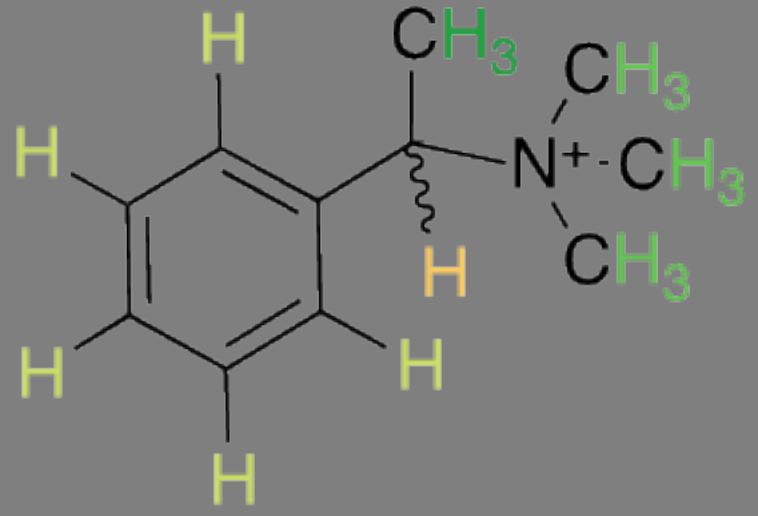

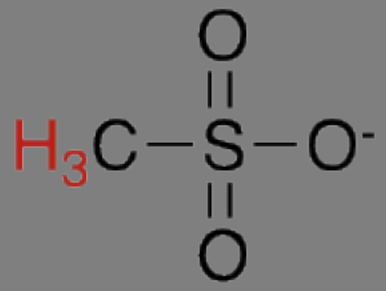

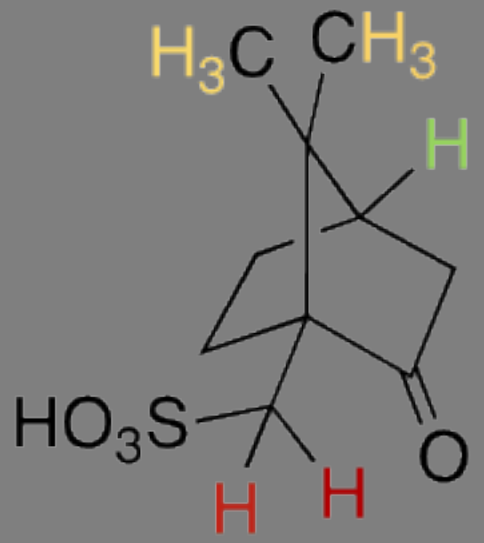

Figure 5: $\Delta\delta_{DESs}$ = differences (in ppm) between the chemical shifts of the signals of +CSA/FR DES and +CSA/FS DES.

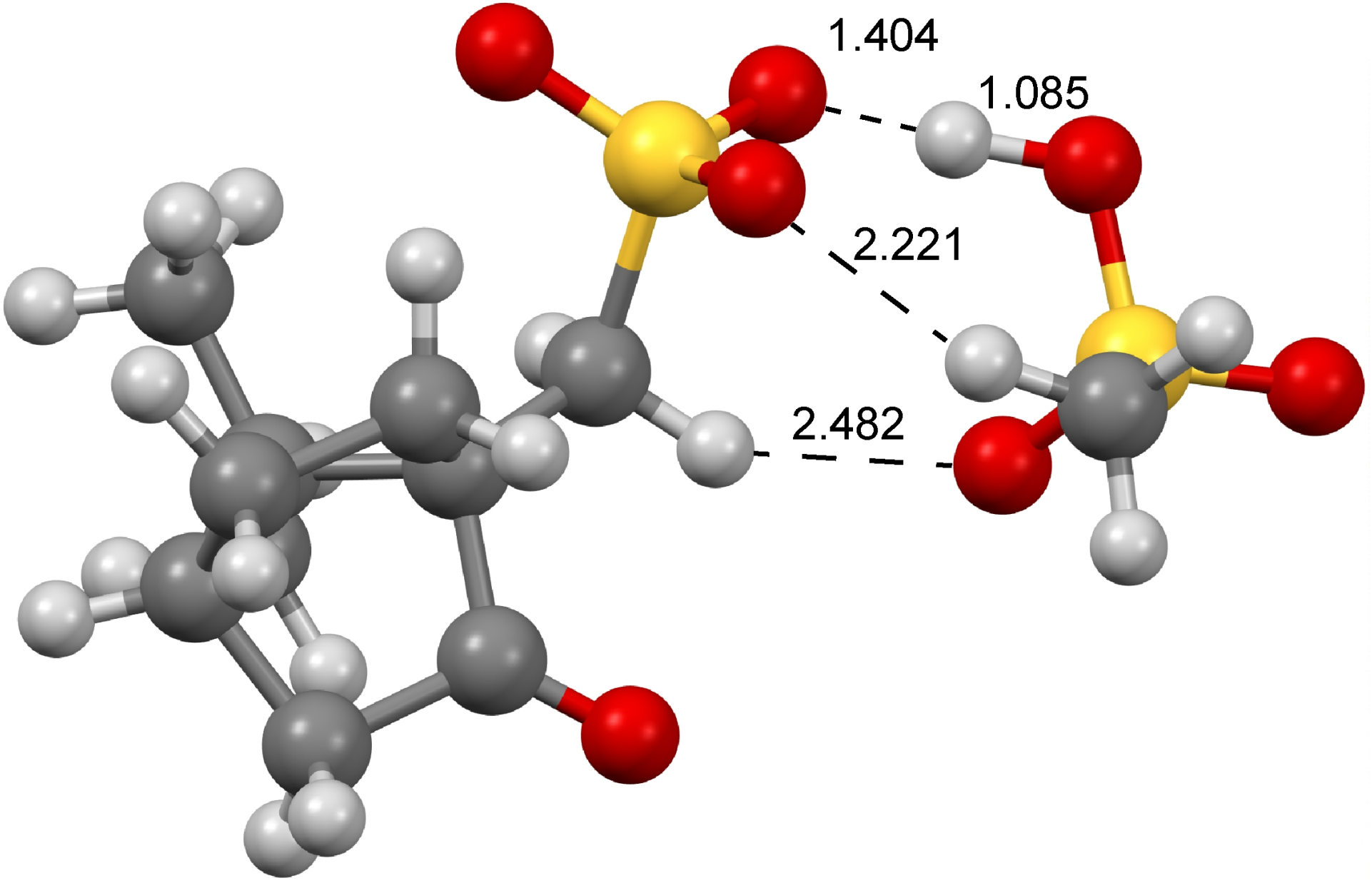
1.404
1.085
2.221
2.482

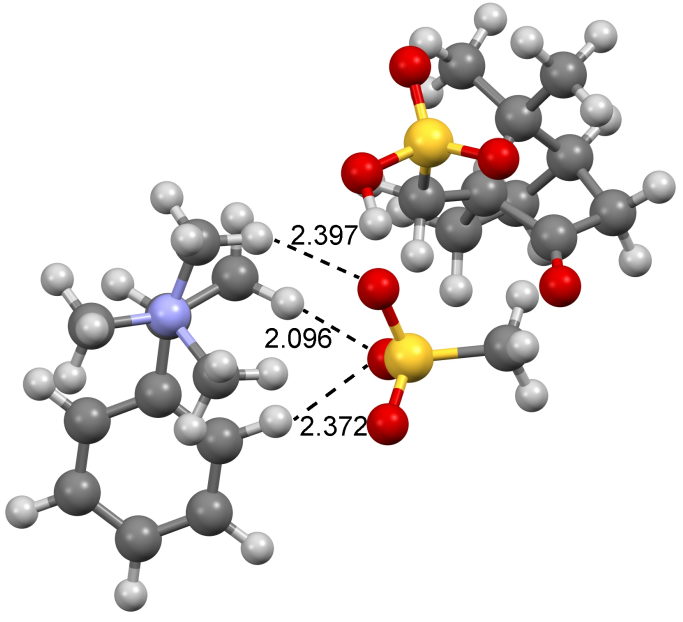

S_Me, E = 6.10

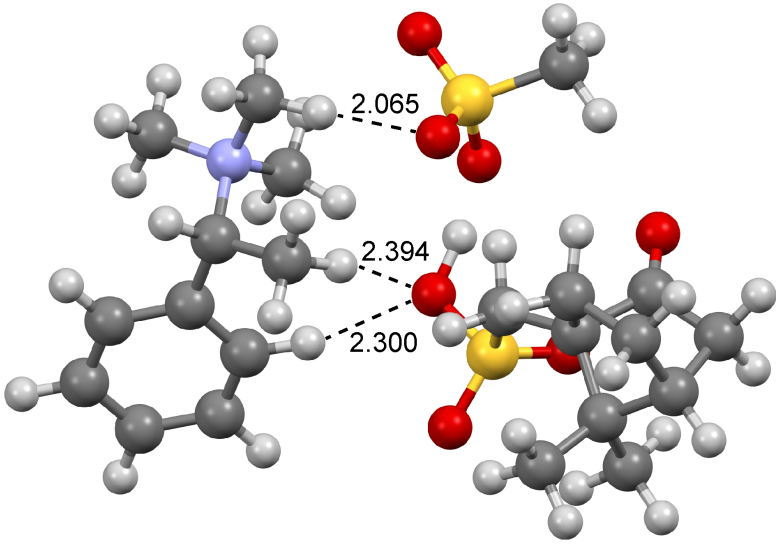

R_Me, E = 2.53

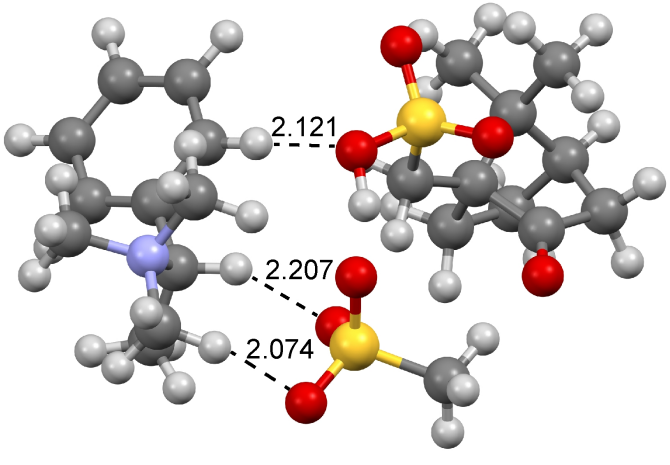

S_CH, E = 0.13

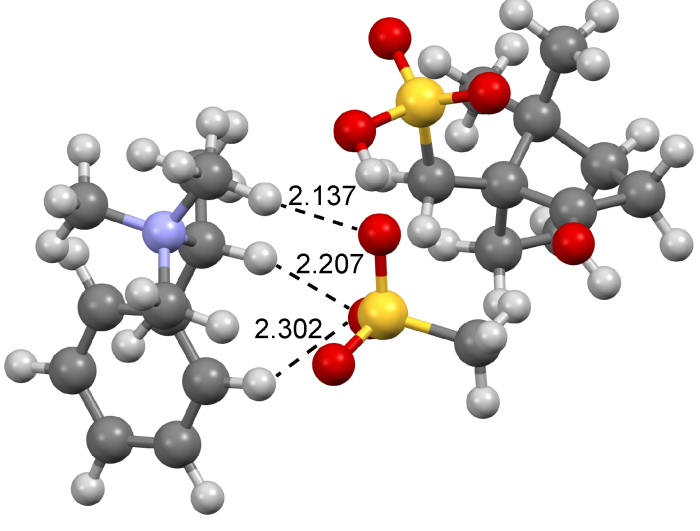

R_CH, E = 0.00

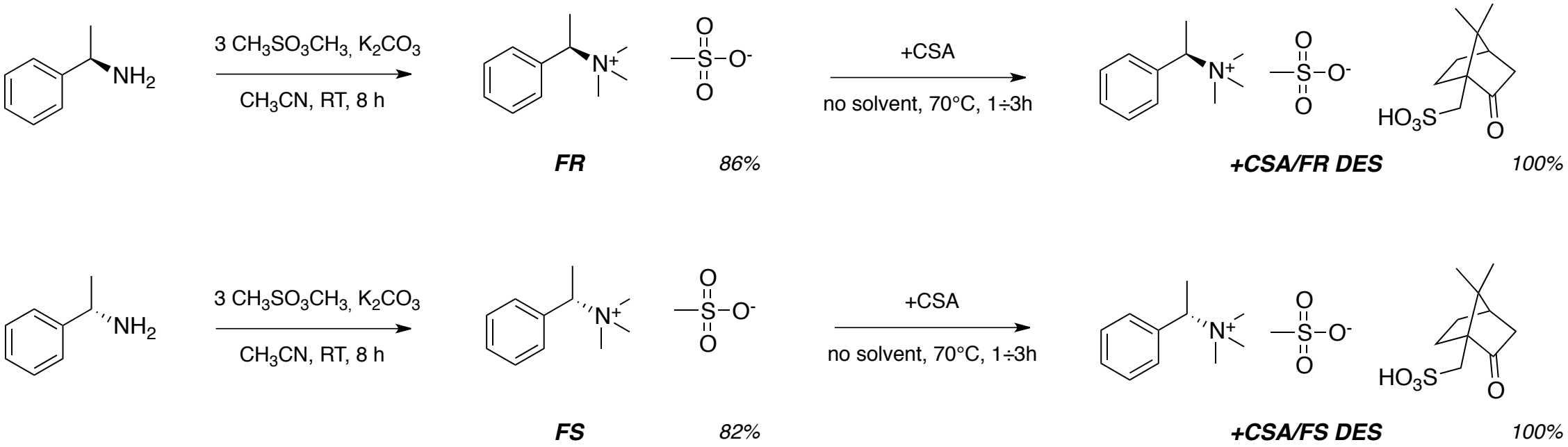

Scheme 1: Chiral DESs realization: synthesis of **(R)- and (S)-**N,N,N-trimethyl-1-phenylethanaminium methanesulfonate (FR and FS) via methylation of the primary amines; mixtures with (1S)-(+)-10-Camphorsulfonic acid to give the DESs.

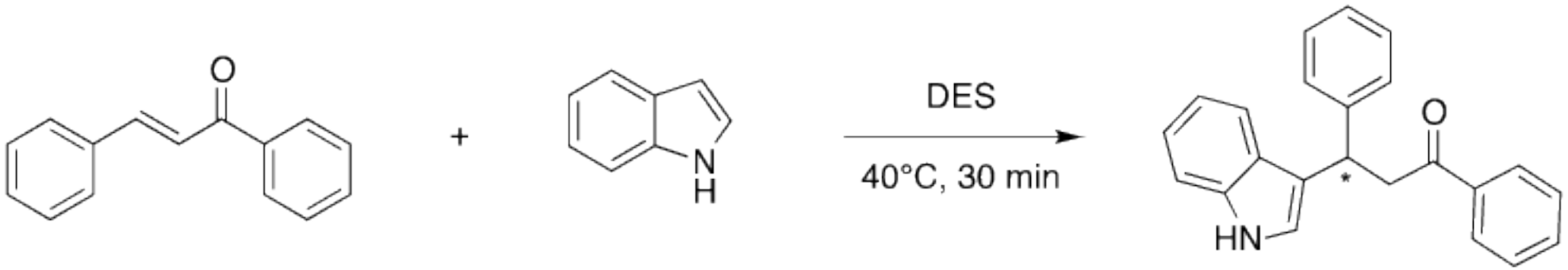

Scheme 2: Michael-Type Friedel-Crafts reaction of indole to chalcone in chiral DESs.

SUPPORTING INFORMATION

Deep Eutectic Solvents formed by chiral components as chiral reaction media and studies of their structural properties

Tommaso Palomba[a], Gianluca Ciancaleoni[b], Tiziana Del Giacco[a], Raimondo Germani[a], Federica Ianni[c], Matteo Tiecco[a]*

[a] Department of Chemistry, Biology and Biotechnology, University of Perugia, Via Elce di Sotto 8 - 06123 Perugia, ITALY.

[b] Department of Chemistry and Industrial Chemistry, University of Pisa, via Giuseppe Moruzzi 13 - 56124 Pisa, ITALY

[c] Department of Pharmaceutical Sciences, University of Perugia, Via del Liceo 1 - 06123, Perugia, ITALY.

* corresponding author. Department of Chemistry, Biology and Biotechnology, University of Perugia, Via Elce di Sotto 8 – 06123 Perugia, ITALY. E-mail: matteotiecco@gmail.com; Tel. +39 075 585 5548; Fax +39 075 585 5560.

INDEX

DESs PREPARATION AND USE AS CHIRAL MEDIA

Figure S1: Eutectic profile of +CSA/FR and +CSA/FS DESs.

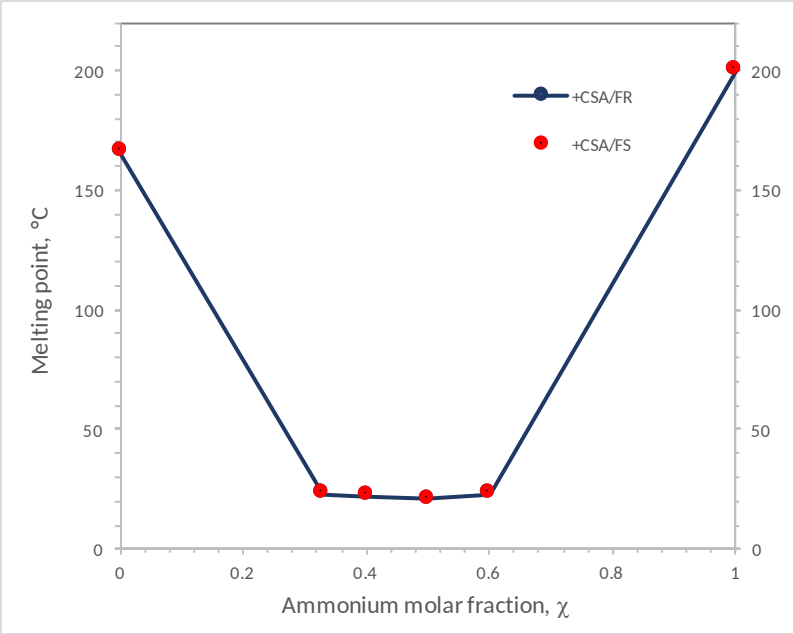

Table S1: Freezing points of the DESs formed by combinations of the enantiomers and the racemates of HBA and HBD molecules used in this work. Molar ratio HBD:HBA = 1:1.

DES	Freezing Point, °C
+CSA/FR	21
+CSA/FS	21
-CSA/FR	21
-CSA/FS	21
+CSA/FRS	18
-CSA/FRS	18
±CSA/FRS	17
±CSA/FR	17
±CSA/FS	17

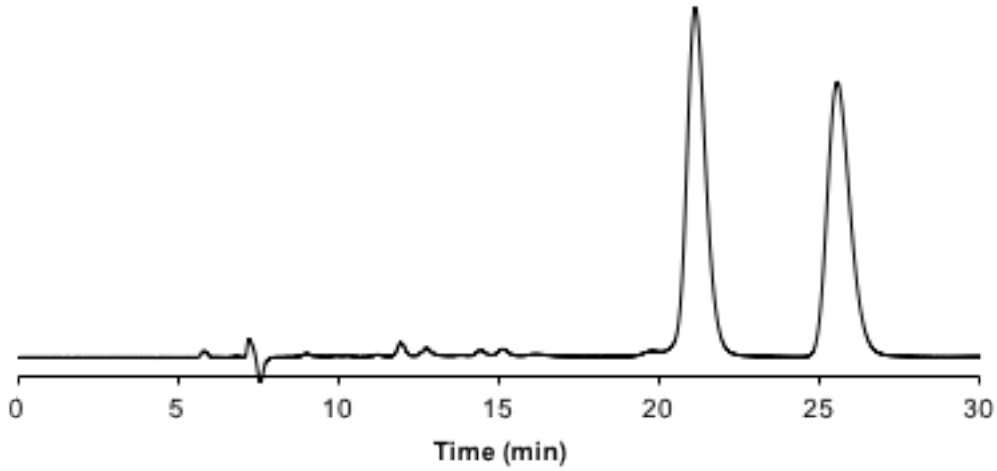

Figure S2: Exemplary chromatogram for the addition products obtained in -CSA/FR DES.

STRUCTURAL PROPERTIES OF THE CHIRAL DESs

DIFFUSION NMR DATA

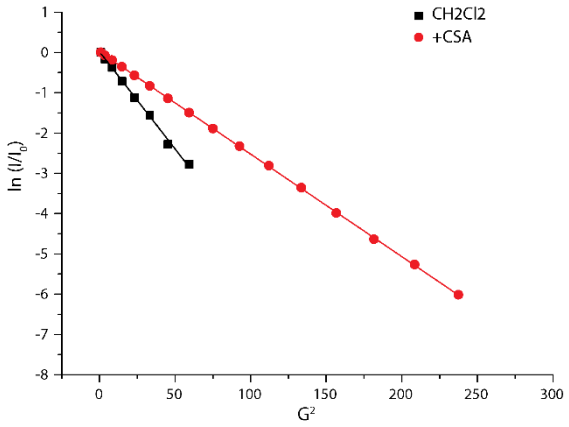

Figure S3. Linear trends of $\ln(I/I_0)$ *vs.* G^2 for a solution containing +CSA (35 mM) and dichloromethane (internal standard).

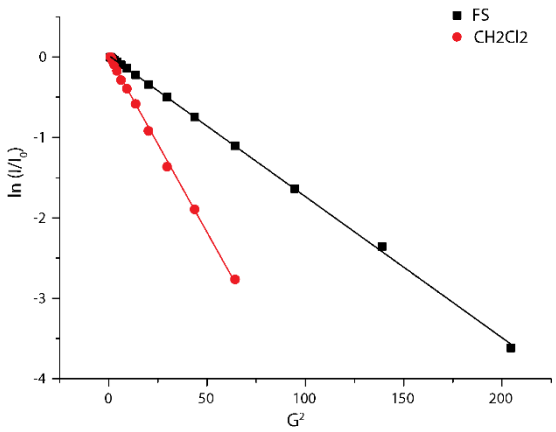

Figure S4. Linear trends of $\ln(I/I_0)$ *vs.* G^2 for a solution containing FS (1.5 mM) and dichloromethane (internal standard).

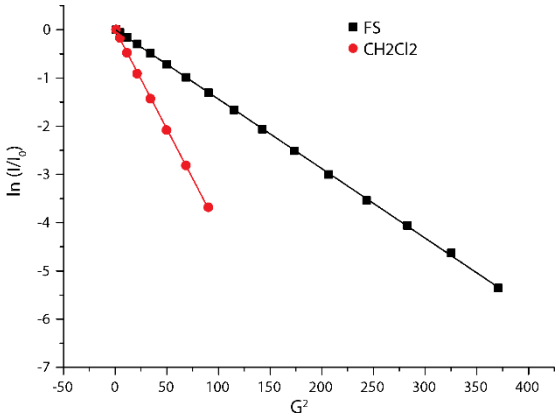

Figure S5. Linear trends of $\ln(I/I_0)$ *vs.* G^2 for a solution containing FS (23 mM) and dichloromethane (internal standard).

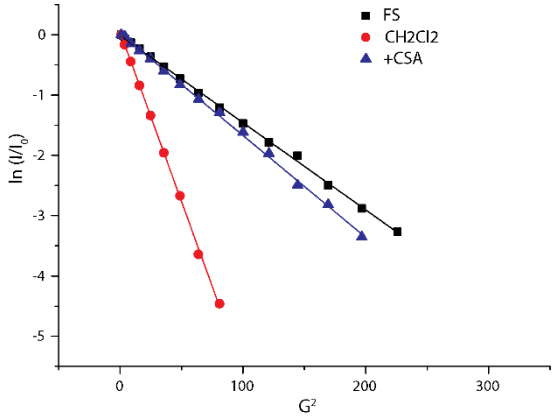

Figure S6. Linear trends of $\ln(I/I_0)$ *vs.* G^2 for a solution containing FS (4 mM), +CSA (4 mM) and dichloromethane (internal standard).

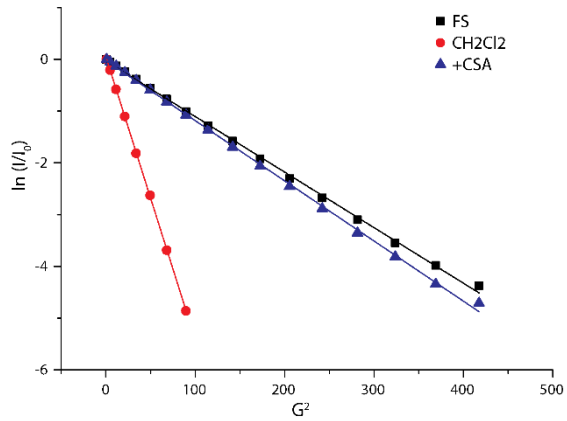

Figure S7. Linear trends of $\ln(I/I_0)$ *vs.* G^2 for a solution containing FS (21 mM), +CSA (21 mM) and dichloromethane (internal standard).

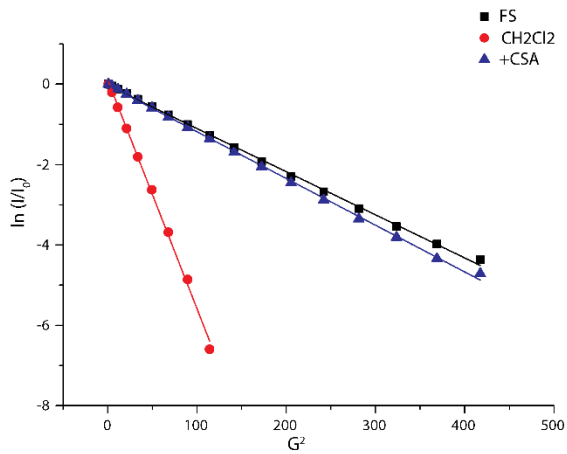

Figure S8. Linear trends of $\ln(I/I_0)$ *vs.* G^2 for a solution containing FS (95 mM), +CSA (95 mM) and dichloromethane (internal standard).

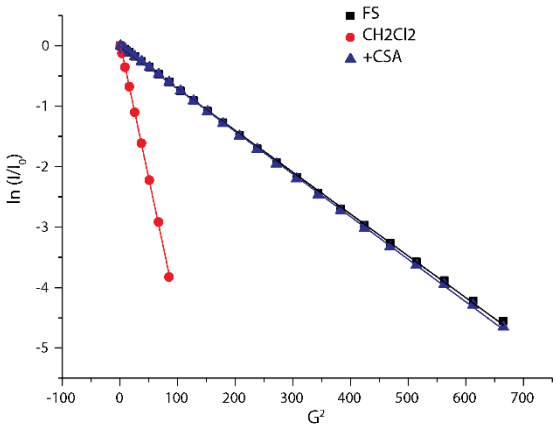

Figure S9. Linear trends of $\ln(I/I_0)$ *vs.* G^2 for a solution containing FS (234 mM), +CSA (234 mM) and dichloromethane (internal standard).

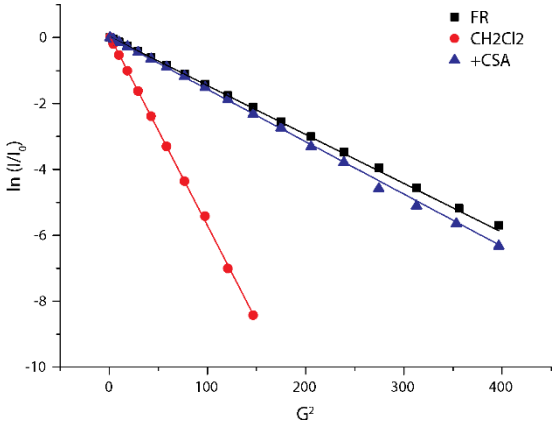

Figure S10. Linear trends of $\ln(I/I_0)$ *vs.* G^2 for a solution containing FR (10 mM), +CSA (10 mM) and dichloromethane (internal standard).

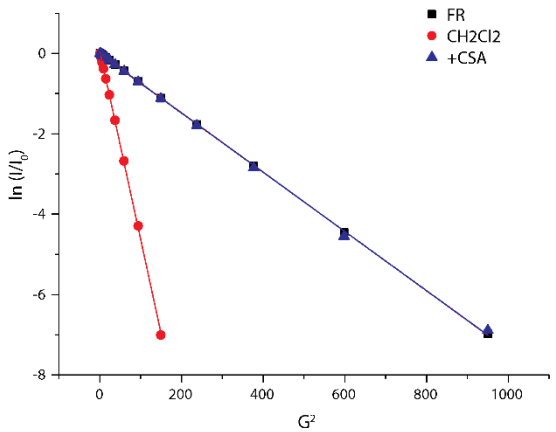

Figure S11. Linear trends of $\ln(I/I_0)$ *vs.* G^2 for a solution containing FR (100 mM), +CSA (100 mM) and dichloromethane (internal standard).

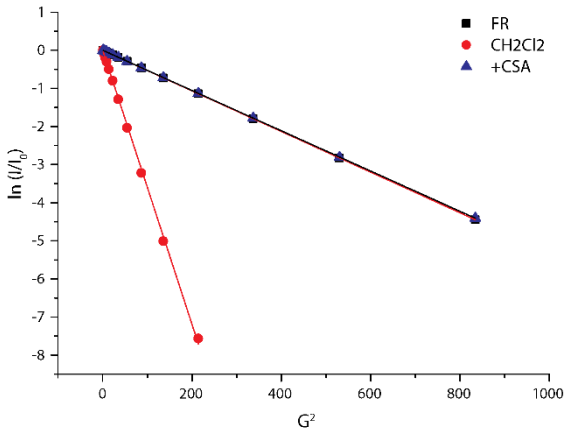

Figure S12. Linear trends of $\ln(I/I_0)$ *vs*. G^2 for a solution containing FR (185 mM), +CSA (185 mM) and dichloromethane (internal standard).

NMR TITRATIONS.

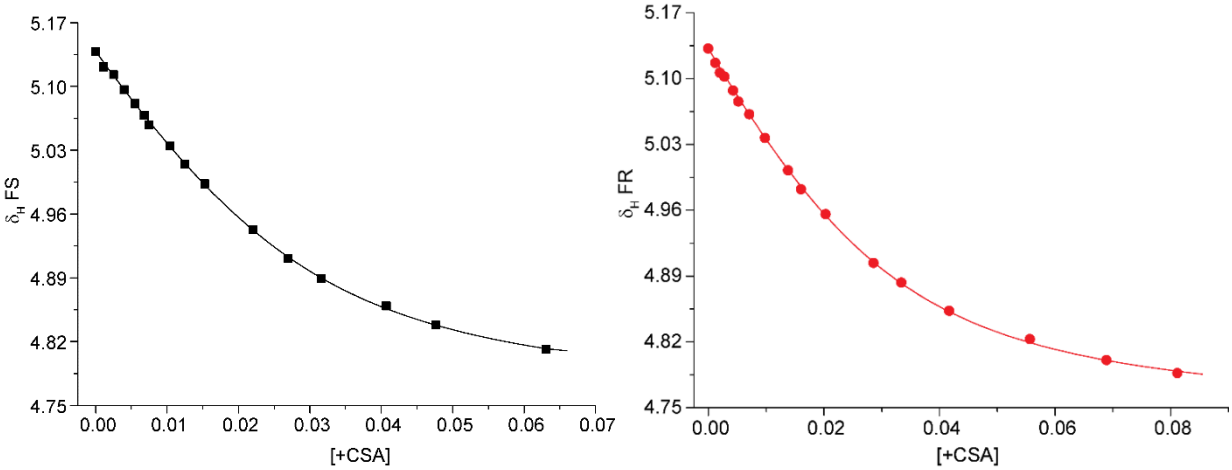

Figure S13: Trends of the chemical shift of the -CH- in the chiral centre for FS (left panel, [FS] = 28.4 mM) and FR (right panel, [FR] = 29.6 mM) with the concentration of +CSA. The limit values of δ (fitted) are 4.749 ± 0.005 and 4.735 ± 0.005 ppm, respectively, and the values of K_f are 131 ± 9 and 115 ± 7 M^{-1}.

Table S2: Chemical shift (□) of N(CH3)3-C*H* signal ([FS] = 28.4 mM) at different [+CSA].

[+CSA] (M)	□ (ppm)
0	5.1385
0.0025	5.1130
0.0075	5.0575
0.0104	5.0347
0.0153	4.9930
0.0221	4.9430
0.0269	4.9110
0.0316	4.8893
0.0407	4.8591
0.0476	4.8383
0.0631	4.8116

Fitting procedure output:

function used for fitting: f(x)
f(x)=deltaA-(deltaA-deltaAB)*0.5*((1+x/ConcA+1/(Kappa*ConcA))-((1+x/ConcA+1/(Kappa*ConcA))**2-4*x/ConcA)**0.5)
fitted parameters initialized with current variable values

iter chisq delta/lim lambda Kappa deltaAB
0 3.6367480047e-05 0.00e+00 1.80e+00 1.386785e+02 4.753710e+00
6 3.4021269177e-05 -3.59e-07 1.80e-02 1.312701e+02 4.749160e+00

After 6 iterations the fit converged.
final sum of squares of residuals : 3.40213e-005
rel. change during last iteration : -3.59296e-012

degrees of freedom (FIT_NDF) : 9
rms of residuals (FIT_STDFIT) = sqrt(WSSR/ndf) : 0.00194426
variance of residuals (reduced chisquare) = WSSR/ndf : 3.78014e-006

Final set of parameters	Asymptotic Standard Error
Kappa = 131.27	+/- 9.289 (7.077%)
deltaAB = 4.74916	+/- 0.005869 (0.1236%)

Table S3: Chemical shift (□) of N(CH3)3-C*H* signal ([FR] = 29.6 mM) at different [+CSA].

[+CSA] (M)	□ (ppm)
0	5.1319
0.0012	5.1165
0.002	5.1063
0.0028	5.1019
0.0043	5.0871
0.0052	5.0755
0.0071	5.0620
0.0098	5.0367
0.0138	5.0024
0.0160	4.9822
0.0203	4.9558
0.0286	4.9037
0.0334	4.8829
0.0417	4.8528
0.0557	4.8227
0.0689	4.8005
0.0812	4.7867

Fitting procedure output:

function used for fitting: f(x)
f(x)=deltaA-(deltaA-deltaAB)*0.5*((1+x/ConcA+1/(Kappa*ConcA))-((1+x/ConcA+1/(Kappa*ConcA))**2-4*x/ConcA)**0.5)
fitted parameters initialized with current variable values
iter chisq delta/lim lambda Kappa deltaAB
0 1.1191908081e-04 0.00e+00 1.63e+00 1.287159e+02 4.744358e+00
5 8.7641255571e-05 -1.77e-01 1.63e-05 1.147644e+02 4.735034e+00

After 5 iterations the fit converged.
final sum of squares of residuals : 8.76413e-005
rel. change during last iteration : -1.7665e-006

degrees of freedom (FIT_NDF) : 15
rms of residuals (FIT_STDFIT) = sqrt(WSSR/ndf) : 0.00241718
variance of residuals (reduced chisquare) = WSSR/ndf : 5.84275e-006

Final set of parameters Asymptotic Standard Error
========== ==========
Kappa = 114.764 +/- 6.658 (5.801%)
deltaAB = 4.73503 +/- 0.004729 (0.09987%)

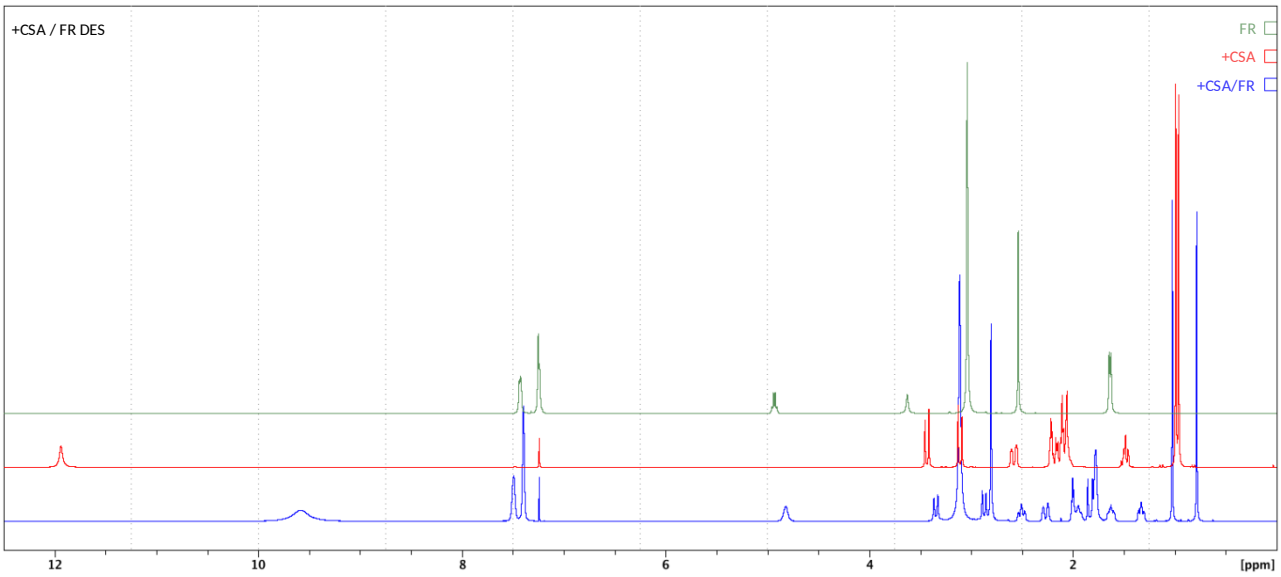

Figure S14: stacked ^{1}H-NMR spectra in $CDCl_3$ of FR (green), +CSA (red) and the +CSA/FR DES (blue) in $CDCl_3$. All the spectra were calibrated on the solvent signal.

Table S4: Chemical shifts (□) of the signals of the pure compounds.

FR		FS		FRS		+CSA		-CSA		±CSA	
Peak	□ [ppm]	Peak	□ [ppm]	Peak	□ [ppm]	Peak	□ [ppm]	Peak	□ [ppm]	Peak	□ [ppm]
1	7.4811	1	7.5279	1	7.5295	1	11.9796	1	5.1081	1	8.2910
2	7.4713	2	7.5179	2	7.5193	2	3.4945	2	3.4945	2	3.4925
3	7.4628	3	7.3697	3	7.5119	3	3.4569	3	3.4569	3	3.4549
4	7.2974	4	7.3597	4	7.3708	4	3.1699	4	3.1588	4	3.1587
5	7.2941	5	7.2830	5	7.3614	5	3.1323	5	3.1214	5	3.1211
6	5.0029	6	5.1004	6	5.0986	6	2.6507	6	2.6474	6	2.6485
7	4.9857	7	5.0834	7	5.0815	7	2.6441	7	2.6405	7	2.6433
8	4.9683	8	5.0661	8	5.0642	8	2.6394	8	2.6397	8	2.6370
9	4.9511	9	5.0492	9	5.0472	9	2.6019	9	2.6029	9	2.6310
10	3.0831	10	3.1698	10	3.1706	10	2.5954	10	2.5969	10	2.6001
11	2.5835	11	2.6750	11	2.6806	11	2.5907	11	2.5930	11	2.5944
12	1.6894	12	1.7556	12	1.7571	12	2.2685	12	2.2235	12	2.5825
13	1.6725	13	1.7390	13	1.7404	13	2.2589	13	2.2589	13	2.2678
						14	2.2482	14	2.2282	14	2.2569
						15	2.2356	15	2.2246	15	2.2460
						16	2.2115	16	2.2105	16	2.2074
						17	2.2004	17	2.2002	17	2.1939
						18	2.1902	18	2.1959	18	2.1756
						19	2.1631	19	2.1786	19	2.1598
						20	2.1492	20	2.1518	20	2.1480
						21	2.1401	21	2.1258	21	2.1279
						22	2.1331	22	2.1025	22	2.1243
						23	2.1009	23	2.1003	23	2.0991
						24	1.5468	24	1.5561	24	1.5522
						25	1.5258	25	1.5345	25	1.5381
						26	1.5037	26	1.5125	26	1.5103
						27	1.4962	27	1.5048	27	1.4991
						28	1.0335	28	1.0442	28	1.0415
						29	1.0057	29	1.0102	29	1.0050

Table S5: Chemical shifts (□) of DESs signals.

+CSA/FR				+CSA/FS				+CSA/FRS			
Peak	**□ [ppm]**	**Peak**	**□ [ppm]**	**Peak**	**□ [ppm]**	**Peak**	**□ [ppm]**	**Peak**	**□ [ppm]**	**Peak**	**□ [ppm]**
1	9.6263	**22**	1.8526	**1**	10.7938	**22**	1.9958	**1**	10.7517	**22**	2.0318
2	7.5350	**23**	1.8225	**2**	7.5313	**23**	1.9885	**2**	7.5287	**23**	2.0112
3	7.4401	**24**	1.7046	**3**	7.4417	**24**	1.9666	**3**	7.4352	**24**	2.0000
4	4.8636	**25**	1.6935	**4**	7.2842	**25**	1.8961	**4**	4.8740	**25**	1.9896
5	3.4088	**26**	1.6818	**5**	4.8671	**26**	1.8502	**5**	4.8628	**26**	1.9818
6	3.3719	**27**	1.6702	**6**	3.4336	**27**	1.8166	**6**	3.4221	**27**	1.9716
7	3.1562	**28**	1.6464	**7**	3.3967	**28**	1.7127	**7**	3.3851	**28**	1.9605
8	2.9349	**29**	1.3961	**8**	3.1530	**29**	1.7012	**8**	3.1471	**29**	1.9526
9	2.8979	**30**	1.3735	**9**	2.9674	**30**	1.6894	**9**	2.9551	**30**	1.8884
10	2.8483	**31**	1.3510	**10**	2.9305	**31**	1.6779	**10**	2.9181	**31**	1.8426
11	2.5774	**32**	1.3430	**11**	2.8740	**32**	1.6669	**11**	2.8622	**32**	1.8113
12	2.5492	**33**	1.0692	**12**	2.5716	**33**	1.6544	**12**	2.5838	**33**	1.7006
13	2.5212	**34**	0.8289	**13**	2.5439	**34**	1.6441	**13**	2.5750	**34**	1.6892
14	2.3357			**14**	2.5152	**35**	1.4037	**14**	2.5472	**35**	1.6775
15	2.2897			**15**	2.3389	**36**	1.3958	**15**	2.5195	**36**	1.6657
16	2.0580			**16**	2.2931	**37**	1.3733	**16**	2.5116	**37**	1.6541
17	2.0477			**17**	2.0609	**38**	1.3508	**17**	2.3297	**38**	1.6420
18	2.0369			**18**	2.0505	**39**	1.3421	**18**	2.3224	**39**	1.6310
19	1.9951			**19**	2.0395	**40**	1.0709	**19**	2.2839	**40**	1.0666
20	1.9667			**20**	2.0177	**41**	0.8315	**20**	2.0533	**41**	0.8241
21	1.8985			**21**	2.0085			**21**	2.0428		

-CSA/FR				-CSA/FS		-CSA/FRS			
Peak	**□ [ppm]**	**Peak**	**□ [ppm]**	**Peak**	**□ [ppm]**	**Peak**	**□ [ppm]**	**Peak**	**□ [ppm]**
1	10.5904	**29**	2.0307	**1**	11.6599	**1**	11.7230	**29**	2.0147
2	7.5268	**30**	2.0095	**2**	7.5339	**2**	7.5272	**30**	2.0037
3	7.5206	**31**	1.9997	**3**	7.4371	**3**	7.5208	**31**	1.9944
4	7.4387	**32**	1.9886	**4**	7.2821	**4**	7.4415	**32**	1.9852
5	7.4331	**33**	1.9799	**5**	4.8792	**5**	4.8743	**33**	1.9751
6	4.8892	**34**	1.9696	**6**	3.4368	**6**	4.8582	**34**	1.9645
7	4.8734	**35**	1.9590	**7**	3.4037	**7**	3.4409	**35**	1.9554
8	4.8565	**36**	1.9504	**8**	3.1524	**8**	3.4038	**36**	1.8921
9	4.8407	**37**	1.8874	**9**	2.9755	**9**	3.1442	**37**	1.8463
10	3.4189	**38**	1.8415	**10**	2.9415	**10**	2.9803	**38**	1.8184
11	3.3817	**39**	1.8159	**11**	2.8794	**11**	2.9613	**39**	1.8046
12	3.1452	**40**	1.8005	**12**	2.5525	**12**	2.9432	**40**	1.7085
13	2.9503	**41**	1.7016	**13**	2.5232	**13**	2.8813	**41**	1.6968
14	2.9132	**42**	1.6898	**14**	2.3336	**14**	2.5789	**42**	1.6850
15	2.8590	**43**	1.6782	**15**	2.2909	**15**	2.5696	**43**	1.6731
16	2.5817	**44**	1.6664	**16**	2.0478	**16**	2.5425	**44**	1.6613
17	2.5726	**45**	1.6546	**17**	1.9912	**17**	2.5145	**45**	1.6494
18	2.5451	**46**	1.6427	**18**	1.8909	**18**	2.5056	**46**	1.6385
19	2.5172	**47**	1.6317	**19**	1.8186	**19**	2.3465	**47**	1.4001
20	2.5088	**48**	1.3964	**20**	1.6699	**20**	2.3366	**48**	1.3909
21	2.3387	**49**	1.3874	**21**	1.3899	**21**	2.3282	**49**	1.3769
22	2.3294	**50**	1.3728	**22**	1.3683	**22**	2.3001	**50**	1.3688
23	2.3210	**51**	1.3653	**23**	1.0717	**23**	2.2912	**51**	1.3603
24	2.2929	**52**	1.3570	**24**	0.8280	**24**	2.2823	**52**	1.3463
25	2.2836	**53**	1.3428			**25**	2.0589	**53**	1.3369
26	2.2752	**54**	1.3333			**26**	2.0481	**54**	1.0698
27	2.0524	**55**	1.0648			**27**	2.0368	**55**	0.8290
28	2.0419	**56**	0.8231			**28**	2.0251		

±CSA/FR				±CSA/FS				±CSA/FRS			
Peak	**□ [ppm]**	**Peak**	**□ [ppm]**	**Peak**	**□ [ppm]**	**Peak**	**□ [ppm]**	**Peak**	**□ [ppm]**	**Peak**	**□ [ppm]**
1	10.1171	**29**	1.9611	**1**	11.1121	**29**	2.0230	**1**	11.2846	**29**	1.8890
2	7.5282	**30**	1.8914	**2**	7.5284	**30**	2.0129	**2**	7.5281	**30**	1.8431
3	7.4350	**31**	1.8455	**3**	7.5214	**31**	2.0020	**3**	7.4364	**31**	1.8179
4	4.8663	**32**	1.8193	**4**	7.4406	**32**	1.9921	**4**	4.8808	**32**	1.8038
5	4.8501	**33**	1.8065	**5**	7.4358	**33**	1.9834	**5**	4.8645	**33**	1.7038
6	3.4120	**34**	1.7002	**6**	7.4279	**34**	1.9726	**6**	3.4318	**34**	1.6922
7	3.3750	**35**	1.6883	**7**	4.8785	**35**	1.9627	**7**	3.3947	**35**	1.6806
8	3.1464	**36**	1.6771	**8**	4.8621	**36**	1.9536	**8**	3.1470	**36**	1.6688
9	2.9416	**37**	1.6654	**9**	3.4300	**37**	1.8894	**9**	2.9684	**37**	1.6571
10	2.9046	**38**	1.6542	**10**	3.3929	**38**	1.8436	**10**	2.9313	**38**	1.6451
11	2.8521	**39**	1.6417	**11**	3.1471	**39**	1.8188	**11**	2.8718	**39**	1.6341
12	2.5806	**40**	1.6311	**12**	2.9658	**40**	1.8042	**12**	2.5851	**40**	1.3974
13	2.5720	**41**	1.3984	**13**	2.9287	**41**	1.7037	**13**	2.5761	**41**	1.3886
14	2.5443	**42**	1.3896	**14**	2.8700	**42**	1.6922	**14**	2.5485	**42**	1.3665
15	2.5161	**43**	1.3751	**15**	2.5849	**43**	1.6803	**15**	2.5206	**43**	1.3440
16	2.5088	**44**	1.3675	**16**	2.5752	**44**	1.6687	**16**	2.5125	**44**	1.3346
17	2.3310	**45**	1.3593	**17**	2.5479	**45**	1.6569	**17**	2.3326	**45**	1.0692
18	2.3228	**46**	1.3451	**18**	2.5203	**46**	1.6451	**18**	2.2868	**46**	0.8264
19	2.2851	**47**	1.3355	**19**	2.5115	**47**	1.6340	**19**	2.0550		
20	2.2772	**48**	1.0652	**20**	2.3428	**48**	1.3983	**20**	2.0448		
21	2.0536	**49**	0.8244	**21**	2.3320	**49**	1.3890	**21**	2.0337		
22	2.0430			**22**	2.3238	**50**	1.3750	**22**	2.0130		
23	2.0319			**23**	2.2969	**51**	1.3668	**23**	2.0017		
24	2.0116			**24**	2.2864	**52**	1.3579	**24**	1.9919		
25	2.0021			**25**	2.2780	**53**	1.3444	**25**	1.9834		
26	1.9901			**26**	2.0556	**54**	1.3345	**26**	1.9732		
27	1.9816			**27**	2.0449	**55**	1.0690	**27**	1.9625		
28	1.9719			**28**	2.0337	**56**	0.8265	**28**	1.9540		

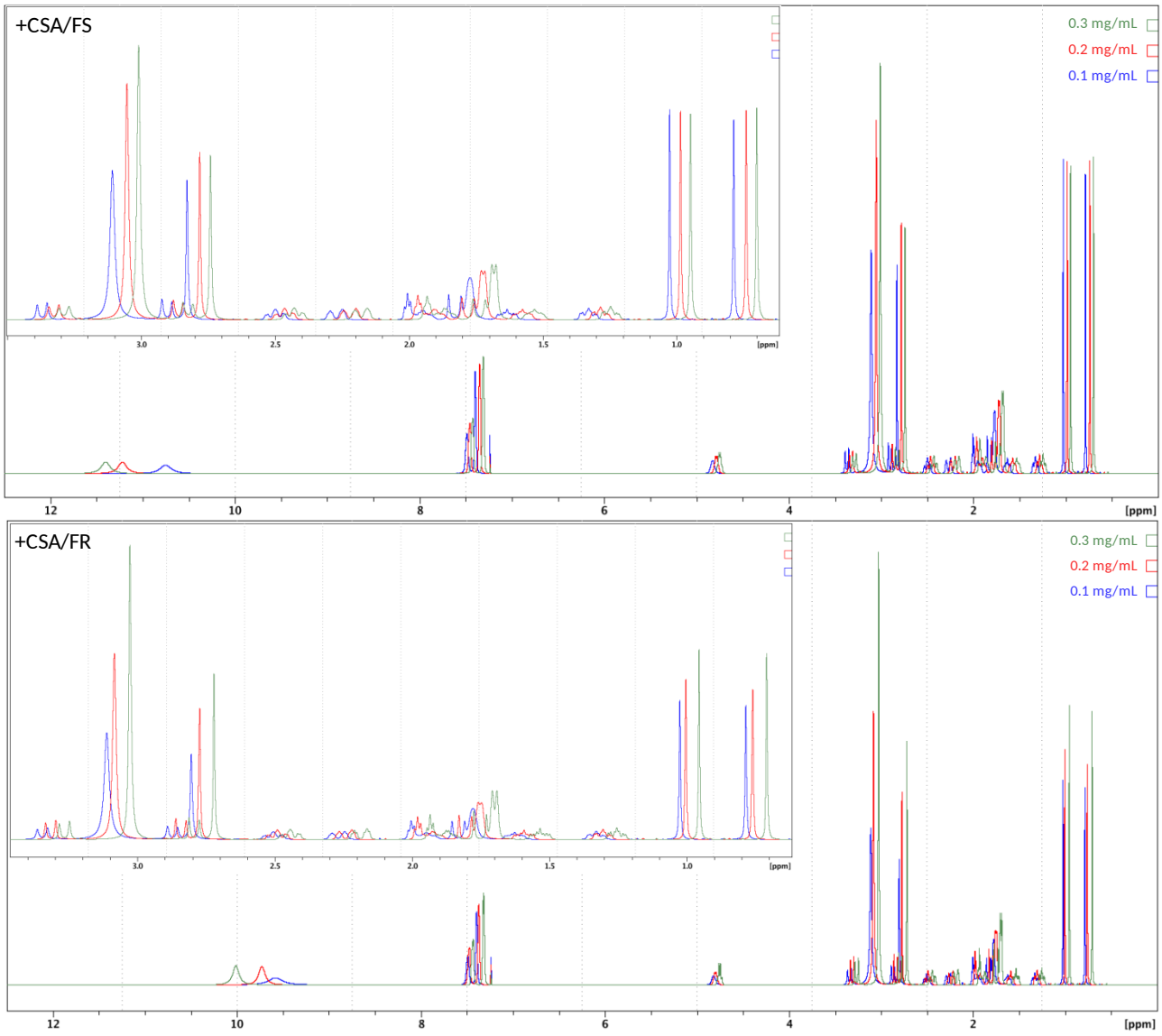

Figure S15: Stacked ^{1}H-NMR spectra of +CSA/FS (up) and +CSA/FR DESs at the concentrations of 0.3 mg/mL (green), 0.2 mg/mL (red) and 0.1 mg/mL (blue) in $CDCl_3$.

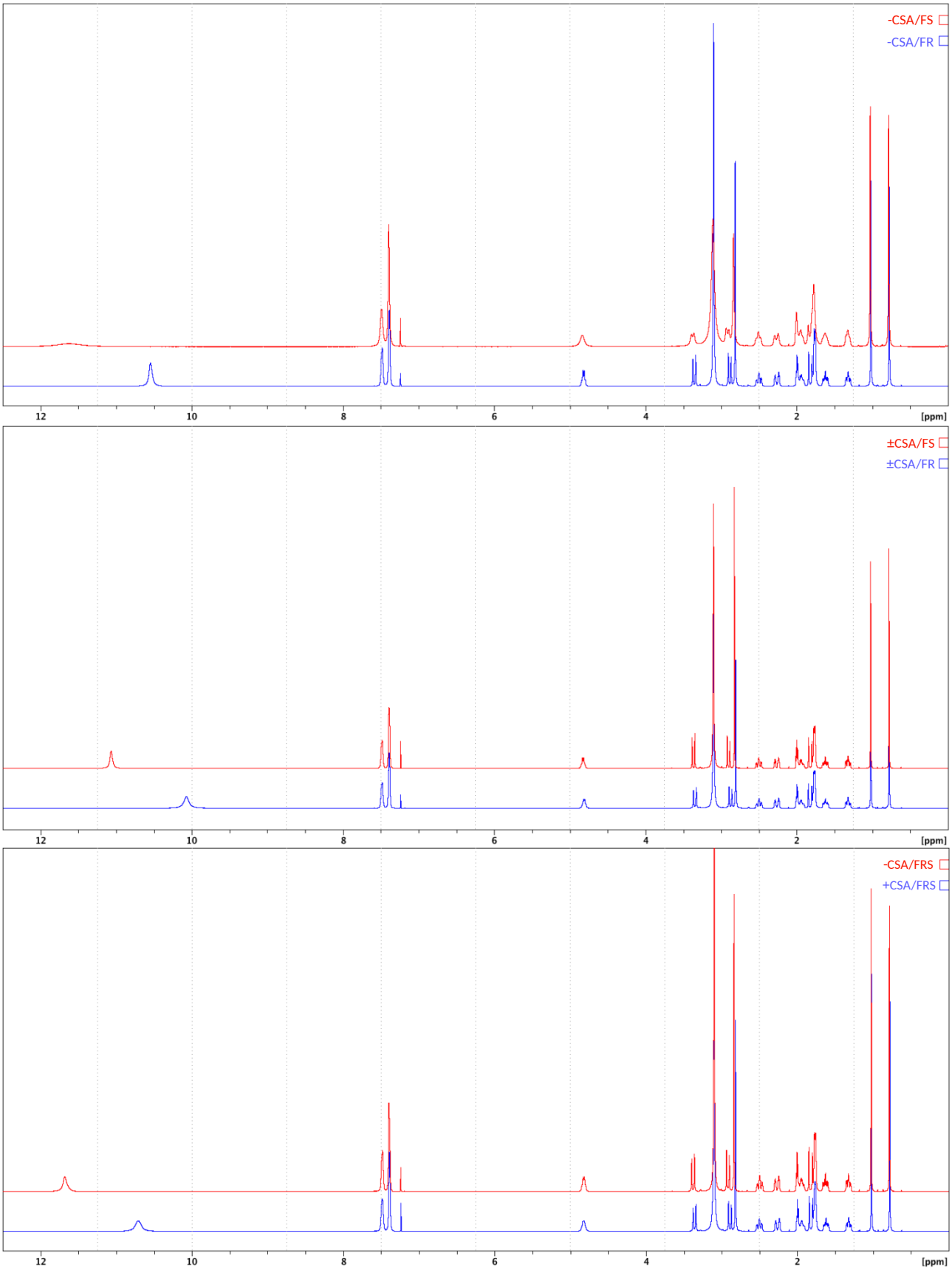

Figure S16: Stacked ^{1}H-NMR spectra in $CDCl_3$ of the DESs couples -CSA/FS -CSA/FR (up); ±CSA/FR ±CSA/FR (middle); -CSA/FRS -CSA/FRS (down). All the spectra are calibrated on solvent signal.

Table S6: $\Delta\delta_{DESs}$ of the analysed DESs couples and the Δ_{yields} of the same couples in the Friedel-Craft probe reaction. In red the most relevant signals of the CSA HBD portion; in blue the most relevant peaks of the ammonium HBA molecules.

SIGNAL	Δδ(+CSA/FR-FS)	Δδ(-CSA/FR-FS)	Δδ(±CSA/FR-FS)	Δδ(+CSA/FRS -CSA/FRS)
H aromatic	0.0011	-0.003	0.011	-0.0102
H benzilic	-0.0035	-0.0142	-0.0121	0.0021
H1 in α at $-SO_3H$	-0.0248	-0.02	-0.018	-0.0188
$(CH_3)_3N^+$	0.0032	-0.0072	-0.0007	0.0029
H2 in α at $-SO_3H$	-0.0326	-0.0267	-0.0242	-0.0252
Methanesulfonate	-0.0257	-0.0204	-0.0179	-0.0191
H in CSA ring	0.0021	-0.01	0.0193	0.0413
Methyl in chiral C	0.0059	-0.0104	0.0014	-0.0002
Methyl 1 geminal	-0.0017	-0.0069	-0.0038	-0.0032
Methyl 2 geminal	-0.0026	-0.0049	-0.0021	-0.0049
Δ_{yields}	**37**	**12**	**2**	**11**

Table S7: Coefficient of determinations of the $\Delta\delta_{DESs}$ of the signals with the Δ_{yields}. In red the most relevant signals of the CSA HBD portion; in blue the most relevant peaks of the ammonium HBA molecules.

SIGNAL	R^2 of correlation with the Δ_{yield}
H aromatic	0.02946
H benzilic	0.14075
H1 in α at $-SO_3H$	0.97558
$(CH_3)_3N^+$	0.17203
H2 in α at $-SO_3H$	0.97548
Methanesulfonate	0.98193
H in CSA ring	0.13313
Methyl in chiral C	0.21908
Methyl 1 geminal	0.29263
Methyl 2 geminal	0.03025

Table S8: DFT studies.

+CSA-Methanesulfonate

C	-0.24910097397974	-0.62297846743679	1.56264216168502
C	-0.10693489904645	-0.91733526787853	0.06852626484873
H	0.40201639783411	-1.87705544167683	-0.08940399549805
H	0.48747072344608	-0.12112060928822	-0.40990006423031
H	-1.06763868412025	-0.99549442781022	-0.45027963997672
C	1.15897754048902	-0.56558052576634	2.17129992159291
H	1.72292313047894	0.28257719663322	1.75238130640351
H	1.71500087779677	-1.48216931064997	1.92748174396871
H	1.16055903594274	-0.47006785954399	3.26557109162218
C	-1.20007162441175	-1.61169969387802	2.32859523548128
C	-1.11702532250689	0.63845523195253	1.86910865500080
H	-0.71817850327711	1.57726944407072	1.45790862777677
C	-1.31625242189300	-0.90154680835597	3.68774231410649
C	-1.22743624433348	0.60837217784321	3.40132842345628
H	-0.34525375645124	1.01949197107895	3.91355559468832
H	-2.11080675753682	1.12803410171342	3.80061562266295
C	-2.59281266806363	-1.27952334358787	1.67915798406540
H	-2.71524080773462	-1.90222376594380	0.78620208470577
H	-3.41803915785084	-1.52996574403844	2.35628453997340
C	-2.50505103124995	0.23423620978963	1.33026596561674
H	-2.58194414450302	0.39754430132401	0.24675316735984
H	-3.30294642337531	0.82442063957721	1.80486386675182
O	-1.48106126533297	-1.40916683083552	4.77868473595404
C	-0.77802804456153	-3.06992701337174	2.44889813008320
H	-0.94668806463469	-3.44244830857465	3.47020344998265
H	0.29434540797707	-3.18501692499374	2.23945482385232
S	-1.60537431315073	-4.25758804180710	1.35389118911878
O	-0.82777893771560	-5.52810768026780	1.58340437528811
H	-1.18155639625798	-6.36895659483714	2.65026345903907
O	-2.99643381111480	-4.34850467272071	1.83069165554981
O	-1.44112046024014	-3.77388349061148	-0.02322815547336
S	-1.48648301693670	-6.41892814295516	4.84075851535738
O	-1.50922308519127	-7.48474340723035	5.83211633074471
O	-1.41795887953417	-7.08811132744512	3.42821786097872
O	-0.48195615514871	-5.36878677003563	4.96535408541121
C	-3.09330935868307	-5.62827309053257	4.83513425659376
H	-3.85698147605763	-6.41280737425605	4.78459148888286
H	-3.15753472973163	-4.97208505811205	3.95595021592696
H	-3.17807169933901	-5.05830527954105	5.76791271064791

R_CH

C	0.19975924999645	-2.02442868272603	1.82207990054436
C	-0.26065765155987	-2.02097134234711	0.35643118139959
H	0.02553948337055	-2.95229038029214	-0.14579705254972

H	0.22710689343998	-1.18726820725286	-0.17200206863772
H	-1.34573942252694	-1.92055699980607	0.23954477789883
C	1.66470923240561	-2.46947868632245	1.85450470909168
H	2.27385606722336	-1.79457812337369	1.23455361879820
H	1.75562504955145	-3.48040987807647	1.43277101009189
H	2.10092900457791	-2.47815231443189	2.86169926724101
C	-0.71094193089069	-2.82009052419295	2.82538589378904
C	-0.06771409029874	-0.65119145519194	2.51889205525236
H	0.43719395339146	0.19857323701119	2.04007286912632
C	0.34500393769399	-0.90478051801495	3.98234792509898
H	1.42935458538808	-0.80181764659793	4.12167468337344
H	-0.14024993008183	-0.19744983839060	4.66828809120038
C	-1.60596677172921	-0.56491840409104	2.50001246506520
H	-2.00454857327776	-0.26398037584662	1.52081681211809
H	-2.03354690971651	0.11322011798754	3.25213630897552
C	-0.86974747821951	-4.32507236840817	2.79789837938362
H	-1.65101590793986	-4.62768081769813	3.51319862021177
H	0.06451717843433	-4.82921986064013	3.08292062636226
S	-1.32435394724227	-5.07746355857149	1.22093000261295
O	-1.86222673229081	-6.49192608794210	1.68728946883359
O	-2.39558447866201	-4.31548512680966	0.60843783434801
O	-0.10659042179688	-5.35028175395697	0.47155462953779
C	-2.01734003530473	-2.01381578508847	2.78811909637126
C	-0.12251939607796	-2.36796718245266	4.21419288251554
H	-0.87334010122193	-2.46915959118059	5.00924499307782
H	0.71368259134927	-3.03074551499445	4.47776264863342
O	-3.13555086447788	-2.41368081727787	3.04236613366225
H	-2.80504997169629	-6.43261449672790	2.17374128180838
S	-4.10563271650686	-6.26539172094744	4.34535832714131
O	-4.75479951676161	-7.32233964010871	5.13697338108319
O	-4.04663478809583	-6.63892825858900	2.88248823469820
O	-2.77292238842018	-5.86697645722626	4.85130419138819
C	-5.13712018570900	-4.81182112476864	4.40090519697276
H	-6.10934495734112	-5.06638363297401	3.96511793231130
H	-4.63594832804732	-4.02261237362056	3.82679045291014
H	-5.24765041343058	-4.52071772690888	5.45156329557444
N	-1.89631434599636	-9.76351117228491	3.85654934005380
C	-2.54643347978955	-9.45480497542820	2.53594936858409
H	-1.77955271836455	-9.22186039118003	1.79376761756943
H	-3.21483967092481	-8.59498834802543	2.66467101991996
H	-3.11450130941685	-10.33994935932914	2.22785280111147
C	-2.99146510595711	-9.98205318385803	4.86507498116895
H	-3.56820974794969	-9.05252618056883	4.98895620328272
H	-2.54230173531946	-10.28619076357211	5.81424388943621
H	-3.64294856437387	-10.77656615809845	4.48178205377789
C	-1.10030557506104	-11.02111062850239	3.73181231982226
H	-0.35281192101126	-10.90404571783087	2.94169537134996
H	-1.78669484806169	-11.83447948603787	3.47142892913001

H	-0.61643736748958	-11.23518881096125	4.68925068215654
C	-0.99753504737546	-8.54495280624401	4.30638333646410
C	-0.56506106092037	-8.69979988452896	5.74759907776930
C	0.19170758857307	-8.90897022728866	8.44523285679874
C	0.55947926805033	-9.45484632522676	6.11731715650978
C	-1.29001592391679	-8.02753793400488	6.74395842030792
C	-0.91312172049560	-8.13424070330094	8.08368705111311
C	0.93156508333094	-9.56532146688086	7.45818121294358
H	1.16983626163873	-9.94525674336435	5.35738901017055
H	-2.13483942501072	-7.40103449270590	6.44989146726992
H	-1.48365169430167	-7.60313037488054	8.84621813581763
H	1.80883815712060	-10.15331460392340	7.73101502424091
H	0.48655442051768	-8.99019108391942	9.49244493697898
C	0.16046561829402	-8.30977917217847	3.34786425139637
H	0.70080766025244	-7.42736880022195	3.71606257877768
H	-0.17575660469903	-8.06697583137725	2.33558480196128
H	0.87920186406397	-9.13871050711232	3.32206437966149
H	-1.69419737290461	-7.69543994831566	4.24950166713974

R_Me

C	0.21747556706432	-1.92185853218884	1.95106363357841
C	0.20790881204040	-2.04661005004932	0.42071582622902
H	0.68866285418343	-2.97987833935126	0.10399672064985
H	0.77770271701610	-1.20920504554042	-0.01144251162128
H	-0.79691381145460	-2.04815860189387	-0.01597263574845
C	1.64380905099344	-2.20568287430027	2.43247104488678
H	2.34304223008950	-1.49321708393480	1.97005439087815
H	1.94763971807975	-3.21508078811886	2.12205717663331
H	1.76376681817720	-2.12925253738547	3.52038703774718
C	-0.87001171206525	-2.75767532994362	2.71554762988803
C	-0.35784337973785	-0.55199045234063	2.43560571950970
H	0.18598697433530	0.32248105001682	2.05381804201414
C	-0.36048663006826	-0.69046990668967	3.97140813034481
H	0.62438593131223	-0.46319187388123	4.40031198826240
H	-1.08339430526949	-0.00889790056230	4.44027554622122
C	-1.82803780937454	-0.62893512427853	1.98009088245402
H	-1.94932451239425	-0.43795252195019	0.90429315418172
H	-2.50849767010561	0.04842463568240	2.51452154057836
C	-0.88252357142716	-4.26871660586828	2.75277905790036
H	-1.78274038344820	-4.61992358422818	3.28089586829188
H	-0.00587335803009	-4.65594160447422	3.29027276964353
S	-0.86681573936589	-5.14269114387656	1.16878420556567
O	-1.47835093294005	-6.54033123918950	1.56933469557725
O	-1.73795879230866	-4.46531358739972	0.22758981927553
O	0.52154253535713	-5.40378666642029	0.80674820568889
C	-2.18121143390188	-2.09047141047724	2.27647074827658
C	-0.73641387330666	-2.18403868648231	4.17610161751138

H	-1.66663871854040	-2.33266757888550	4.74074911400257
H	0.05119275188589	-2.73830785474566	4.70521974880809
O	-3.29141298558132	-2.58311969078574	2.28896565096502
H	-2.54716885734982	-6.49614986623643	1.81433061439091
S	-4.16212833400905	-6.45488190907768	3.66641997663434
O	-4.87472528552667	-7.60571748872073	4.23505051296015
O	-3.85217165992245	-6.65617025204041	2.20069563223360
O	-2.94489014349314	-6.06458496007190	4.42118270961216
C	-5.25686404880802	-5.04587603938708	3.69185434699691
H	-6.15065117259759	-5.30080115841521	3.11185485640536
H	-4.72582637259067	-4.19927969152851	3.23904340439556
H	-5.51906716195549	-4.84015347299195	4.73571817143104
N	-1.43771926729220	-9.51262950845309	4.56062140949910
C	-2.16982766611476	-9.26824722160423	3.27089827098186
H	-1.78166307877341	-9.95053430627974	2.50989834356825
H	-2.01451218284992	-8.23445177879166	2.96212891680799
H	-3.23930575289956	-9.42365799301299	3.44719225186548
C	-2.16469381064147	-8.81862664775427	5.68028999579061
H	-2.32261060956956	-7.76615819321670	5.41255914298788
H	-1.57025676905927	-8.92755293560934	6.59587765057309
H	-3.14481693343276	-9.29222349209571	5.79345268236511
C	-1.43395099528314	-10.98317893491209	4.82961734795966
H	-0.86696912759557	-11.48926433627765	4.04228123030895
H	-2.47204340876201	-11.33255871126819	4.83289127862150
H	-0.97572847201289	-11.16901950087074	5.80818712541717
C	0.04543080389907	-8.99271228645621	4.49377492496101
C	0.10187520102133	-7.47131930974722	4.50857636693264
H	1.15285616278719	-7.18071122212075	4.38403060520896
H	-0.26549339989260	-7.04681988346641	5.44824486484637
H	-0.46832260225505	-7.02602064681524	3.68518176711117
H	0.47166737894668	-9.39112893863366	5.42738318757678
C	0.78804028642434	-9.60441954131290	3.32768277394083
C	2.22235075820903	-10.74551505345917	1.20137863743320
C	0.75243035859245	-9.01707823193165	2.05278095726537
C	1.56906902717996	-10.75294191997051	3.52752470540692
C	2.28037245873620	-11.32489229235836	2.47149319114756
C	1.46363776126552	-9.58971875473306	0.99803508491710
H	0.17683600234756	-8.10885239237706	1.87076765675357
H	1.63182854840283	-11.19537077784636	4.52440780070318
H	2.88505001641934	-12.21620535124548	2.64240538845633
H	1.42812618018586	-9.11717963486275	0.01615532444030
H	2.77916982705520	-11.18693443450360	0.37401607289809

S_CH

C	-0.03113632286503	-1.78810280123521	1.61769303513995
C	-0.77259055877071	-1.61482091841208	0.28292753033935
H	-0.60956344635327	-2.48226245742590	-0.36675627876171

H	-0.38157502515480	-0.72421747053990	-0.23385105364336
H	-1.85715487095794	-1.50441028743968	0.39652978899656
C	1.39721123794975	-2.24727879403876	1.30939822307948
H	1.90076956777417	-1.50382714818292	0.67239791281410
H	1.36957938183604	-3.19591107962112	0.75438866005216
H	2.01447839547768	-2.39134236526189	2.20539126670460
C	-0.75219550914335	-2.68540391294827	2.68666540003072
C	-0.11216118100038	-0.50136823191075	2.50074994004091
H	0.31572090953203	0.39278367882856	2.02800118274539
C	0.57067929807118	-0.92558013513091	3.81616484632119
H	1.66397880063754	-0.85105005453975	3.74789414311405
H	0.25263821611593	-0.29528727593874	4.65793208332726
C	-1.62098392341037	-0.39934040851463	2.79695530772084
H	-2.19476414023412	0.02064087793670	1.95884461094150
H	-1.87012958832371	0.18817050586650	3.69240442373886
C	-0.95112357071092	-4.17812028979489	2.52724060683429
H	-1.57240471573201	-4.55831176326409	3.35379455364988
H	0.01097844653599	-4.70843015930849	2.55800361512121
S	-1.73205610600723	-4.74747744377407	1.00478765334458
O	-2.15538650033050	-6.22429512659963	1.39128375841240
O	-2.90846420182555	-3.94658784971606	0.72666618562200
O	-0.69908550580047	-4.89821380108469	-0.01064400925671
C	-2.01471646326584	-1.86831556082778	2.99262420543710
C	0.10962689716981	-2.40025339900026	3.97359394575962
H	-0.47695097075267	-2.58340881073081	4.88370631603208
H	0.95824053543916	-3.09856987531663	3.99303026032363
O	-3.07884415542108	-2.28347936693322	3.40501597301183
H	-2.95357908714163	-6.28551821924586	2.09079893873972
S	-3.78120994564387	-6.29366264170315	4.50873252700699
O	-4.30156612044489	-7.33768520290635	5.40675891636491
O	-3.93477879449843	-6.71743213355105	3.06192892200383
O	-2.39657463506698	-5.87435598641901	4.80130359084462
C	-4.81628839576762	-4.85224247433353	4.68097275921492
H	-5.83540306826473	-5.12552941569873	4.38611935524235
H	-4.41046561209182	-4.05997542184222	4.03938108866354
H	-4.78605871944596	-4.54621642077494	5.73308058608754
N	-1.92973512515424	-9.86978615202385	3.64711003791046
C	-2.34038097626020	-9.48114638684533	2.25435049131791
H	-1.44666788218665	-9.24999825298460	1.66904369012767
H	-2.99265655431607	-8.60253033161871	2.32439849320819
H	-2.87604335881981	-10.32792551469220	1.80992709458979
C	-3.18233855722691	-10.10684678972216	4.44473429070869
H	-3.71458559538579	-9.15635034877496	4.60013724544988
H	-2.91265921519249	-10.54299002366161	5.41097870203680
H	-3.80350386663393	-10.81255764957052	3.88126435638827
C	-1.14032229514699	-11.13828388408566	3.59334020552587
H	-0.28271428324955	-11.00228403073143	2.92893053325147
H	-1.79392188272368	-11.93377642107878	3.21775044496784

H	-0.79170359502948	-11.38977357412484	4.60018188249441
C	-1.08529838628676	-8.69134161464526	4.27539981215586
H	-1.66583650598503	-7.79946469636752	4.00787374523878
C	-1.04874435431136	-8.77525942903251	5.79321870525519
H	-0.40185679851968	-7.96161611109804	6.14372487474869
H	-0.63584808215345	-9.72066917356352	6.17431625540519
H	-2.04042950039604	-8.59720521024126	6.22272818486319
C	0.27510094294428	-8.59112947793878	3.62194647463043
C	2.79422255779446	-8.29407540462004	2.40832530320502
C	0.43328995558726	-7.77436071460658	2.49229001566654
C	1.40155786886029	-9.24367220264530	4.14670558140343
C	2.65131099373974	-9.09948220157806	3.54258557414281
C	1.68279946634302	-7.62952934506573	1.88577929813335
H	-0.42839433674814	-7.23909507077727	2.08955088741076
H	1.31084799278722	-9.85696363024832	5.04477808595364
H	3.51860461596879	-9.60894565941369	3.96425689235556
H	1.77700634028091	-6.98769316425734	1.00911674139697
H	3.77320986530702	-8.17855789265194	1.94134532889507

S_Me

C	-0.16482454600927	-1.61783953732270	1.62744603608246
C	-1.12354376693838	-1.39493472911511	0.44738557987593
H	-1.06143643371535	-2.22155695942138	-0.26893259635155
H	-0.84488214538963	-0.46681841078759	-0.07696747843993
H	-2.17477928668211	-1.31903893322859	0.75022851363231
C	1.19973535388424	-2.02834351760915	1.06839043800962
H	1.58536279093404	-1.23701725153579	0.40671290821438
H	1.09507147498568	-2.94391651322105	0.47023881759236
H	1.95355120981067	-2.20974801244107	1.84557766662731
C	-0.69644953564480	-2.57448727913397	2.75918206124892
C	-0.11809304678348	-0.37068590110386	2.57028081823367
H	0.22040492250613	0.54884500733830	2.07442245772107
C	0.77140321578392	-0.83540795260154	3.73771909014766
H	1.83789523765840	-0.74768948605034	3.49170869372018
H	0.59562212270888	-0.24178147915157	4.64557028422781
C	-1.56011561709012	-0.30658468564892	3.10692603423284
H	-2.26333118097988	0.15967040621044	2.40309618453227
H	-1.66156639067388	0.21840965481646	4.06773640944789
C	-0.90551764130987	-4.06905250574440	2.58823652559566
H	-1.50006092600388	-4.45332228966554	3.43425657697402
H	0.05735187363454	-4.59753152532450	2.56336153142770
S	-1.76175464940977	-4.63709375777827	1.10649173462473
O	-1.96195538119269	-6.16614306432658	1.42665239391843
O	-3.04936209634861	-3.96721626553212	1.02030027137675
O	-0.83917047517974	-4.57214412678686	-0.01631152012900
C	-1.91451658591403	-1.79026112137440	3.26945473162668

C	0.35067139213819	-2.31974077576053	3.90684739543015
H	-0.08265005346595	-2.54449256572596	4.89107263051947
H	1.19946442020750	-3.00292350765961	3.76472956988839
O	-2.92175297018065	-2.24303817737975	3.77231646702594
H	-2.81652743463600	-6.34979739930447	2.06279168684498
S	-4.05454646133807	-6.17844806538513	4.22980271945721
O	-4.84342514538620	-7.04422369177091	5.11105634297790
O	-3.83908934542566	-6.85104930846977	2.88250753689838
O	-2.76217699124850	-5.73348479018966	4.80031345950057
C	-5.00634871212094	-4.71702824141415	3.86769071816953
H	-5.96256421548219	-5.03993732328809	3.44154672507419
H	-4.44045971133791	-4.10123074779542	3.15948041664333
H	-5.15701294902372	-4.17337569489970	4.80657638330923
N	-1.59694776319691	-9.82518761256602	3.85716287490268
C	-1.78893420185608	-9.50440777685878	2.40241761960178
H	-0.82787487738050	-9.59752020995370	1.88577729523893
H	-2.18933442860254	-8.49157070822950	2.30511439757605
H	-2.50836551737644	-10.22214386886328	1.99243937443491
C	-2.88385994918552	-9.54772785508723	4.58314687199188
H	-3.08084521451856	-8.47592888647518	4.61093423382274
H	-2.81513312219913	-9.94646167294447	5.59818115749317
H	-3.69290794717536	-10.03375122648290	4.02837495430161
C	-1.28450782344965	-11.28102772440953	3.99604630348266
H	-0.40504454677755	-11.52141636228387	3.38782126110670
H	-2.14972312578073	-11.85729502178947	3.65002227414282
H	-1.08633754370468	-11.49922060585556	5.04996907910204
C	-0.37823510155394	-8.99655168462506	4.44542251734316
H	0.48285477944312	-9.57288954283511	4.07394206933069
C	-0.33102974618728	-7.58139970913478	3.89581477072315
H	0.50824406908168	-7.07258414904817	4.38897804221174
H	-1.23870587909185	-7.00554941221932	4.12506427968272
H	-0.15851654866597	-7.54703492320032	2.81505976401122
C	-0.38880890743665	-9.04618422373639	5.95475673217296
C	-0.37779093689947	-9.15081612305868	8.75932186867844
C	0.37518261914753	-10.00910422454338	6.63049212902471
C	-1.13055970216217	-8.11296101890125	6.70009578323355
C	-1.12680789612125	-8.17561271966878	8.09370676211673
C	0.38183387856462	-10.06471312952241	8.02592465009632
H	0.99080388808530	-10.70975495918997	6.06038553277821
H	-1.71546317688139	-7.33578797905223	6.20105681005345
H	-1.71243804519150	-7.45128983200522	8.66064622843368
H	0.98520429817131	-10.81517814641220	8.53813248072015
H	-0.37657185043926	-9.19046816546402	9.84989566628161

FS

S	-4.03607752695816	-6.36936917273019	4.14195938284235
O	-4.97202600255676	-7.51946394089973	4.15063270978583
O	-3.15734026457055	-6.35745051481398	2.94425553025061
O	-3.27581643911185	-6.23448014224274	5.40855304322117
C	-5.05669949391625	-4.89566152455007	4.01818922178688
H	-5.63825614645486	-4.95606557537994	3.09097899142230
H	-4.39638315530986	-4.02111863182833	4.00315087236324
H	-5.72145395206358	-4.86210364382983	4.88913290504127
N	-2.00036167753124	-9.71442792839299	3.98432020385520
C	-2.58313590307829	-9.42782380363793	2.62389197624058
H	-1.79429280593406	-9.53241346439197	1.87233066123439
H	-2.99506517506731	-8.40691765089601	2.62212723770050
H	-3.37349307784128	-10.16306368663762	2.43996692509316
C	-3.13807464214652	-9.90960853892447	4.94997143690476
H	-3.80486822533880	-9.03419552487543	4.89266497232789
H	-2.72380586324408	-10.03712537361250	5.95378117787157
H	-3.68189617425125	-10.81275519912240	4.64618236666921
C	-1.20048719597496	-10.97396041179801	3.92131134049974
H	-0.33653465590773	-10.82255922881792	3.26647126171005
H	-1.83844502708310	-11.76491788615707	3.51111638483089
H	-0.86806241930086	-11.24049464721816	4.92840238749968
C	-1.13424406822427	-8.48774582044993	4.45795424430823
C	-0.53990082784803	-8.72803415290704	5.82549495963792
C	0.52208349571852	-9.05959741709333	8.40483634727726
C	0.65823641184166	-9.43404449953690	6.01895377040799
C	-1.18475145372440	-8.16282800319836	6.93732771839722
C	-0.65580173466760	-8.33217621017286	8.21884927885047
C	1.18287310545466	-9.60547437600669	7.30078162174950
H	1.20064329361494	-9.84239808041058	5.16448014042461
H	-2.08695790368713	-7.56719049787797	6.77345479451911
H	-1.16315011784329	-7.88401843548056	9.07383450419801
H	2.11557837504989	-10.15417032168076	7.43674525319942
H	0.93532141768369	-9.18847174434482	9.40618292889846
C	-0.12398695774876	-8.07083007780089	3.39912419233533
H	0.44440269699019	-7.22808708045036	3.81278695548027
H	-0.62602089025797	-7.70608223982439	2.49644326499899
H	0.59948655138784	-8.85621903374360	3.13691794252812
H	-1.88023557009858	-7.68565551826359	4.55044109363784

+CSA

C	-2.65809097594715	-2.76623150182415	4.52317091951794
C	-2.02789206474498	-1.81016412106264	5.53798629199548
H	-0.99167425916067	-1.57540267065141	5.26271521382044
H	-2.01709966848725	-2.28508079664039	6.53102716961174
H	-2.55777855538899	-0.85567363698278	5.62479925365978
C	-1.79082737334604	-4.03018338569454	4.45260322629889

H	-1.80842429698307	-4.55859820985907	5.41689081106683
H	-0.74212517561696	-3.76693347862828	4.25014013260397
H	-2.10523791651636	-4.73862330480869	3.67436994546358
C	-2.93366570191731	-2.13998090556473	3.11106993834700
C	-4.17102790867040	-3.05057810226757	4.80022718513067
H	-4.37168525368335	-3.52084807318256	5.77142321212765
C	-3.77549677255273	-3.26230663416858	2.45994717069156
C	-4.59352132136248	-3.89466301667439	3.58615763951376
H	-4.32662105087820	-4.95771336827989	3.67271043083405
H	-5.66765084641106	-3.84883130016689	3.35624173092993
C	-4.00992713561132	-1.04893650900635	3.43223987191446
H	-3.51544056670419	-0.11642359734612	3.72903315172753
H	-4.62279550793471	-0.81567779794338	2.55282458306064
C	-4.81911816702774	-1.66232376277676	4.61173414837168
H	-4.73025968738723	-1.04667461751384	5.51545635305293
H	-5.88978969590710	-1.74835332162687	4.38234447521387
O	-3.78420587039107	-3.56262136239256	1.28369384395800
C	-1.76568934950985	-1.77713892854426	2.20851009759366
H	-2.02305487594364	-2.02254710389443	1.16559043900984
H	-0.85744709478496	-2.33254065241154	2.47992569125273
S	-1.28074997791066	-0.04941787806572	2.18954826092350
O	0.05003008718292	-0.13846929824034	1.24210464051090
H	-0.21899405395490	0.16605498380532	0.35197112694061
O	-2.27059398234557	0.73437714675166	1.47307152763451
O	-0.81092498010300	0.34730520566174	3.49637151722187